HAL open science

The abnormal accumulation of heparan sulfate in patients with mucopolysaccharidosis prevents the elastolytic activity of cathepsin V

Thibault Chazeirat, Sophie Denamur, Krzysztof Bojarski, Pierre-Marie Andrault, Damien Sizaret, Fuming Zhang, Ahlame Saidi, Marine Tardieu, Robert Linhardt, François Labarthe, et al.

To cite this version:

Thibault Chazeirat, Sophie Denamur, Krzysztof Bojarski, Pierre-Marie Andrault, Damien Sizaret, et al.. The abnormal accumulation of heparan sulfate in patients with mucopolysaccharidosis prevents the elastolytic activity of cathepsin V. Carbohydrate Polymers, 2021, 253, pp.117261 -. 10.1016/j.carbpol.2020.117261 . hal-03677275

HAL Id: hal-03677275

https://hal.science/hal-03677275

Submitted on 24 Oct 2022

HAL is a multi-disciplinary open access archive for the deposit and dissemination of scientific research documents, whether they are published or not. The documents may come from teaching and research institutions in France or abroad, or from public or private research centers.

L'archive ouverte pluridisciplinaire **HAL**, est destinée au dépôt et à la diffusion de documents scientifiques de niveau recherche, publiés ou non, émanant des établissements d'enseignement et de recherche français ou étrangers, des laboratoires publics ou privés.

Distributed under a Creative Commons Attribution - NonCommercial 4.0 International License

Version of Record: https://www.sciencedirect.com/science/article/pii/S014486172031434X
Manuscript_72f9f7ff9cba8662eccaca34485246cf

The abnormal accumulation of heparan sulfate in patients with mucopolysaccharidosis prevents the elastolytic activity of cathepsin V

Thibault Chazeirat[1,2], Sophie Denamur[1,2,3], Krzysztof K. Bojarski[4], Pierre-Marie Andrault[5], Damien Sizaret[6], Fuming Zhang[7], Ahlame Saidi[1,2], Marine Tardieu[3], Robert J. Linhardt[7], François Labarthe[3,8], Dieter Brömme[5], Sergey A. Samsonov[4], Gilles Lalmanach[1,2], Fabien Lecaille[1,2,¶]

[1] Université de Tours, Tours, France.
[2] INSERM, UMR 1100, Centre d'Etude des Pathologies Respiratoires (CEPR), Team "Mécanismes protéolytiques dans l'inflammation", Tours, France.
[3] Pediatric Department, Reference Center for Inborn Errors of Metabolism ToTeM, CHRU Tours, France.
[4] Faculty of Chemistry, University of Gdańsk, Poland.
[5] Department of Oral Biological and Medical Sciences, University of British Columbia, Vancouver, British Columbia, Canada.
[6] Anatomical Pathology and Cytology department, Bretonneau Hospital, CHRU Tours, France.
[7] Center for Biotechnology and Interdisciplinary Studies, Rensselaer Polytechnic Institute, Troy, New York, USA.
[8] INSERM, UMR 1069, Nutrition, Croissance et Cancer (N2C), Tours, France.

TC : thibault.chazeirat@etu.univ-tours.fr; SD: sophie.denamur@gmail.com; KKB: krzysztof.bojarski@ug.edu.pl; P-MA: andrault_pm@yahoo.fr; DZ: D.SIZARET@chu-tours.fr; FZ : zhangf2@rpi.edu; AS : ahlame.saidi@univ-tours.fr; MT : M.TARDIEU@chu-tours.fr; R-JL : linhar@rpi.edu; FL : francois.labarthe@univ-tours.fr; DB : dbromme@dentistry.ubc.ca; SAS : sergey.samsonov@ug.edu.pl; GL : gilles.lalmanach@univ-tours.fr; FL : fabien.lecaille@univ-tours.fr

¶Corresponding author: Fabien Lecaille, PhD, Université de Tours, INSERM, UMR 1100, CEPR, 10 Boulevard Tonnellé, F-37032 Tours cedex, France. Tel: (+33) 247366083; e-mail: fabien.lecaille@univ-tours.fr

Running title: Regulation of cathepsin V activity by heparan sulfate

© 2020 published by Elsevier. This manuscript is made available under the CC BY NC user license
https://creativecommons.org/licenses/by-nc/4.0/

Abstract:

Mucopolysaccharidosis (MPS) are rare inherited diseases characterized by accumulation of lysosomal glycosaminoglycans, including heparan sulfate (HS). Patients exhibit progressive multi-visceral dysfunction and shortened lifespan mainly due to a severe cardiac/respiratory decline. Cathepsin V (CatV) is a potent elastolytic protease implicated in extracellular matrix (ECM) remodeling. Whether CatV is inactivated by HS in lungs from MPS patients remained unknown. Herein, CatV colocalized with HS in MPS bronchial epithelial cells. HS level correlated positively with the severity of respiratory symptoms and negatively to the overall endopeptidase activity of cysteine cathepsins. HS bound tightly to CatV and impaired its activity. Withdrawal of HS by glycosidases preserved exogenous CatV activity, while addition of Surfen, a HS antagonist, restored elastolytic CatV-like activity in MPS samples. Our data suggest that the pathophysiological accumulation of HS may be deleterious for CatV-mediated ECM remodeling and for lung tissue homeostasis, thus contributing to respiratory disorders associated to MPS diseases.

Keywords: protease, glycosaminoglycan, MPS, lung, elastin

Abbreviations:

AEBSF : 4-(2-aminoethyl) benzenesulfonyl fluoride hydrochloride; CA-074 : N-(L-3-trans-propylcarbamoyloxirane-2-carbonyl)-L-isoleucyl-L-proline; Cat : cathepsin, CS : chondroitin sulfate; DMMB : 1,9-dimethylmethylene blue; DS : Dermatan sulfate; DTT: dithiothreitol, E-64 : trans-epoxysuccinyl-L-leucylamido(4-guanidino)butane; ECM : extracellular matrix, EDTA : ethylenediaminetetraacetic acid; GAG : glycosaminoglycan; GlcA : glucuronic acid; GlcNAc : *N*-acetyl-D-glucosamine; GRSS : global respiratory symptoms severity; HA : hyaluronic acid; HS : heparan sulfate; IF : Immunofluorescence; KS : keratan sulfate; MD : molecular dynamics; MMP : matrix metallo-proteinase; MMTS : *S*-methyl thiomethanesulfonate; MPS : mucopolysaccharidosis; PAS : periodic acid schiff; PMSF : phenylmethylsulfonyl fluoride; ProCat : procathepsin; SPRI : surface plasmon resonance imaging; Surfen : bis-2-methyl-4-amino-quinolyl-6-carbamide hydrate; Z-Phe-Arg-AMC : Z-Phe-Arg-7-amido-4-methylcoumarin.

1. Introduction

Mucopolysaccharidoses (MPS) are a group of seven rare inherited metabolic diseases associated with deficiencies in enzymes involved in the degradation of glycosaminoglycans (GAGs). MPS type I (MPS-I) is a lysosomal disease caused by a deficiency of the α-L-iduronidase, which is essential to correct the metabolism of both dermatan sulfate (DS) and heparan sulfate (HS). MPS-I is commonly classified into three clinical syndromes from severe to attenuated form: Hurler, Hurler-Scheie, and Scheie. MPS-II (or Hunter syndrome) is caused by a deficiency of lysosomal iduronate-2-sulfatase, which is critical for the degradation of both HS and DS, by cleaving their O-linked sulfate. MPS-III (also named Sanfilippo syndrome) is caused by a deficiency in one of the four enzymes involved in the degradation of HS and is divided into four subtypes : heparan N-sulfatase (type IIIA), α-N-acetylglucosaminidase (type IIIB), acetyl CoA: α-glucosaminide acetyltransferase (type IIIC), and N-acetylglucosamine-6-sulfatase (type IIID) (Stapleton et al., 2018). The subsequent accumulation of these GAGs participates in cellular dysfunction, resulting in progressive multi-visceral and tissue damages (Muenzer, 2011). The hallmarks of most MPS-I, II, and III phenotypes are represented by a wide spectrum of clinical severity, including cardiorespiratory diseases, which for the most severe forms of MPS diseases remain the leading cause of early mortality (Arn et al., 2015; Berger et al., 2013; Muhlebach et al., 2011). Thickened depositions/secretions in airways and interstitium due to an abnormal accumulation of extracellular matrix (ECM) components can further exacerbate obstruction (Batzios et al., 2013; Leighton et al., 2001; Pal et al., 2018; Rutten et al., 2016). Under these circumstances, the exact molecular mechanisms by which GAG accumulation ultimately leads to lung disease manifestations have not been clearly elucidated (Iozzo & Gubbiotti, 2018). Therefore, a better understanding of factors affecting airways dysfunction may lead to novel strategies for improving respiratory function in patients with MPS.

Lysosomal cysteine cathepsins are papain-like proteases (eleven members in human: cathepsins B, C, F, H, L, K, O, S, V, X and W) that play key roles in numerous physiological processes in particular the degradation and recycling of endocytosed bulk protein (Lecaille et al., 2002). Beside their expression in endolysosomal system, cathepsins are also found in cytosol or nucleus and can be secreted (Reiser et al., 2010; Vidak et al., 2019). Cathepsins participate in ECM remodeling by degrading major structural proteins (e.g., collagens I, II and IV and elastin), specialized adhesion proteins (e.g., fibronectin, fibrillin, and laminins) and proteoglycan (aggrecan) (Vizovišek et al., 2019). Their uncontrolled proteolytic activity (e.g., protease/inhibitor and redox imbalance) is associated with various human diseases including

118 cardiovascular diseases, immune defects, bone and cartilage diseases (osteoporosis,
119 rheumatoid arthritis), cancer, and lung inflammatory pathologies (emphysema, fibrosis,
120 asthma, chronic obstructive pulmonary disease) (for review: Brömme & Wilson, 2011;
121 Lalmanach et al., 2020). Moreover cathepsins are relevant biomarkers and promising
122 therapeutic targets for numerous diseases (Kramer et al., 2017; Vizovišek et al., 2020).
123 Cathepsins B, C, H, and L are ubiquitously found in mammalian tissues while cathepsins S,
124 K, W, and notably cathepsin V (CatV) exhibit a more restricted expression pattern. CatV (also
125 called CatL2) that shares 80% protein sequence identity with human CatL is mostly expressed
126 in cornea, testis, epidermis, colon, and thymus (Adachi et al., 1998; Brömme et al., 1999;
127 Santamaría et al., 1998; Tolosa et al., 2003). Deficiency in murine CatL, the orthologue of
128 human CatV, induces myocardial fibrosis probably due to a reduced collagenolytic activity
129 (Spira et al., 2007). A 2-fold reduction of CatV protein level was detected in bronchoalveolar
130 lavage fluids of patients with pulmonary sarcoidosis compared to healthy subjects, suggesting
131 an association to lung matrix homeostasis under physiological and pathological conditions
132 (Naumnik et al., 2014). Human CatV displays a 3-fold higher elastolytic activity than CatK
133 and CatS (Yasuda et al., 2004). In addition, GAGs including chondroitin 4-/6-sulfate (C4-S
134 and C6-S), heparin (Hep) and DS decreased *in vitro* the elastolytic activities of both CatV and
135 CatK and to a lesser extent CatS. Similarly, the digestion of type II collagen by CatK is
136 impaired by the presence of high HS and DS concentrations in osteoclasts from MPS-I mouse
137 model, which likely contributes to MPS-I bone pathology (Wilson et al., 2009). Previous
138 reports demonstrate that abnormal expression and/or activity of cathepsins B, S, and K
139 correlate with major clinical manifestations in MPS (for review: De Pasquale et al., 2020).
140 Nevertheless, it remains unknown whether cysteine cathepsins, and especially elastolytic
141 CatV, contribute to respiratory disorders in MPS.
142
143 **Hypotheses**
144 The proteolytic activity of some cysteine cathepsins is tightly controlled by the formation of a
145 complex between their highly positively charged exosites and specific GAGs (for review:
146 Novinec et al., 2014). Our hypothesis is that i*n situ* HS levels in patients with MPS interfere
147 with the proper elastolytic activity of CatV and that this inhibition could be prevented. To
148 address this issue, we evaluated the protein level of CatV and the HS content in respiratory
149 secretions (sputum and tracheal aspirates) of patients with MPS-I, II, and III and unaffected
150 individuals. Also, we characterized CatV elastolytic activity in the presence of HS. Finally,

151 we demonstrated that Surfen, a small HS antagonist, markedly restored the endogenous
152 elastolytic CatV-like activity in MPS samples.

153 **2. Material and methods:**

154 2.1. Reagents- Benzyloxycarbonyl-Phe-Arg-7-amino-4-methyl coumarin (Z-Phe-Arg-AMC)
155 was purchased from R&D Systems (R&D Systems Europe, Abingdon, UK). E-64 (l-3-
156 carboxy-*trans*-2–3-epoxypropionyl-leucylamido-(4-guanidino)-butane), Pepstatin A, EDTA,
157 4-(2-aminoethyl) benzenesulfonyl fluoride hydrochloride (AEBSF, Pefabloc), *S*-methyl
158 thiomethanesulfonate (MMTS) and Elastin-Congo Red conjugate were obtained from Sigma-
159 Aldrich (Saint Quentin Fallavier, France). CatB inhibitor N-(L-3-trans-
160 propylcarbamoyloxirane-2-carbonyl)-L-isoleucyl-L-proline (CA-074) and CatL inhibitor (*N*-
161 (4-biphenylacetyl)-S-methylcysteine-(D)-Arg-Phe-β-phenethylamide, a.k.a CatL inh. 7)
162 (Chowdhury et al., 2002) were from Calbiochem (Merck Millipore, France). CatS inhibitor
163 (morpholinourea-leucinyl- homophenylalanine-vinyl-sulfone phenyl inhibitor, LHVS) was a
164 kind gift from Dr. J. H. McKerrow (Skaggs School of Pharmacy and Pharmaceutical
165 Sciences, University of California, San Diego, USA). Odanacatib (CatK inhibitor) was from
166 Selleck Chemicals (Houston, TX, U.S.A.). Heparan sulfate (HS) from bovine kidney (~14
167 kDa), chondroitin 4-sulfate (C4-S) from bovine trachea (20-30 kDa), chondroitin 6-sulfate
168 (C6-S) from shark cartilage (~63 kDa), dermatan sulfate (DS) from porcine intestinal mucosa
169 (~14 kDa), dermatan sulfate (DS) from porcine intestinal mucosa (~14 kDa), heparin (Hep)
170 from porcine intestinal mucosa (15-17 kDa), hyaluronic acid (HA) from *Streptococcus equi*
171 (~1400 kDa) were from commercial source (Sigma-Aldrich). Perlecan isolated from basement
172 membrane extract (derived from Engelbreth-Holm-Swarm mouse sarcoma) and aggrecan
173 from bovine articular cartilage were supplied by Sigma-Aldrich. Insoluble elastin from bovine
174 neck was a kind gift from Dr. Laurent Duca (UMR CNRS 7369 MEDyC, Reims, France).
175 Surfen (bis-2-methyl-4-amino-quinolyl-6-carbamide hydrate) came from Sigma-Aldrich.
176

177 2.2. Enzymes- Heparinases I, II, III, Δ-4,5-glycuronidase, and chondroitinase B, all from
178 *Flavobacterium heparinum* were purchased from Grampenz (Upper Ardoe, Aberdeen,
179 Scotland). Dnase I from bovine pancreas was purchased from Sigma-Aldrich. Recombinant
180 human procathepsin V (proCatV) was cloned in the pPic9K yeast expression system and
181 expressed in *Pichia pastoris* as previously described (Brömme et al., 1999). The K20G CatV
182 mutant was generated with the following primers, forward: 5'-
183 AAGAATCAGGGACAGTGTGGTTCTTGTT-3', and reverse: 5'-

184 CACTGGCGTCACGTAGCCTT-3', using the pPic9K vector carrying the wild-type proCatV
185 sequence as a template. The expression of the recombinant wild-type (wt) CatV and K20G
186 CatV mutant, extraction, as well as renaturation, purification and processing into active form
187 were carried out as previously described (Du et al., 2013). Unless stated otherwise, enzymatic
188 assays for cathepsin activity were carried out in 100 mM sodium acetate buffer, pH 5.5
189 containing 2 mM dithiothreitol (DTT). Cathepsin activity was recorded using as substrate Z-
190 Phe-Arg-AMC (λ_{ex}=350 nm, λ_{em}=460 nm, Spectramax Gemini spectrofluorometer, Molecular
191 Devices, Saint Grégoire, France). The active site concentrations of wild-type CatV and K20G
192 CatV mutant were determined using E-64 (Barrett et al., 1982).
193
194 2.3. MPS-I lung biopsy- Postmortem lung tissue samples from a 2-year old female with MPS
195 type I were kindly provided by Dr Michael McDermott (Department of Histopathology,
196 Dublin, Ireland). Autopsy findings suggested a cardiopulmonary pathology in combination
197 with transplant related pulmonary venopathy (Gupta et al., 2013). Samples were further used
198 for staining, immunohistological (IHC) and immunofluorescence (IF) examinations.

199 2.4. Lung biological samples from MPS and non-MPS patients- Sputum and tracheal aspirates
200 (respiratory specimens) from MPS patients (N=11, including 2 MPS-I, 5 MPS-II, and 4 MPS-
201 III) and non-MPS patients (controls, N=9) were collected in the Pediatric and Intensive Care
202 Units of the University Hospital of Tours, France. Respiratory-related disorders were
203 evaluated by three independent clinicians for MPS patients as part of routine follow-up. Based
204 on the analysis criteria from early comprehensive literature surveys (Berger et al., 2013;
205 Muhlebach et al., 2011), a global respiratory symptoms severity (GRSS) evaluation was
206 assessed for each patients regarding four sub-types: ear-nose-throat symptoms (chronic
207 rhinitis or sinusitis, otitis, adeno-tonsillar hypertrophy, hearing loss, macroglossia, stridor),
208 pulmonary symptoms (dyspnea, wheezing, cough, sputum, asthma, bronchitis, pneumonia),
209 clinical symptoms of obstructive sleep apnea, and skeletal abnormalities causing restrictive
210 lung disease (scoliosis, kyphosis, ribcage narrowing, chest wall deformity). The GRSS was
211 graduated from 0 to 4, corresponding to the number of respiratory disorder sub-types reported
212 for each patient. This study was approved by the French National bioethical authorities (n°ID-
213 RCB: 2019-A01361-56) and informed written consent was obtained from parents of each
214 participant. Non-MPS patients were intubated for cardiac surgery or severe head trauma.
215 None of the patients in the control group had chronic respiratory disease before admission or
216 breathing symptoms during hospital stay. Tracheal aspirations of MPS and control groups

217 were taken during an orotracheal intubation of the patient in the operating room or in the
218 Pediatric Intensive Care Unit (University Hospital of Tours, France). Samples were
219 aseptically weighed, instantly diluted at 1 g/10 mL in a preservative buffer (100 mM sodium
220 acetate, pH 5.0 plus the peptidase inhibitors 0.5 mM PMSF, 0.5 mM EDTA, 40 µM pepstatin
221 A, and 1 mM MMTS) (Naudin et al., 2011), then centrifuged for 10 min at 5,000 g at 4°C.
222 Resulting cell-free supernatants were collected, aliquoted and stored at -80°C. The total
223 protein quantification of supernatants was performed by BCA assay (ThermoFisher
224 Scientific).

225 2.5. Immunohistological and immunofluorescence studies in MPS-I lung tissue sections-
226 Samples were fixed in neutral-buffered, 10% formalin solution and processed by standard
227 methods for further histological examinations. Conventional immunohistochemistry was
228 performed on automatic BenchMark XT (Roche). The lung parenchyma was stained with
229 Hematoxilin-Eosin-Safran (HES) (Tissue-Tek Prisma, Sakura Finetek Europe). Periodic Acid
230 Schiff (PAS) was used to detect polysaccharides. In parallel, anti-CD68 (a monocyte and
231 macrophage marker, 1:200, Dako) was used as control. Finally, digital microscopic images
232 were acquired from scanned slides (Hamamatsu Nanozoomer 2.0RS, magnification: x200 to
233 x400) and processed with the Hamamatsu NDP.view 2.0 software. The immunohistochemical
234 detections of CatV and HS were obtained without antigen retrieval after removing paraffin
235 with xylene. Tissue sections were rehydrated by sequential washings with ethanol and water.
236 Briefly, the endogenous peroxidase activity was blocked by incubating sections in 3% H_2O_2
237 solution for 20 min. Non-specific binding sites were blocked with 5% BSA in PBS for 1 h at
238 room temperature. Sections were then incubated overnight at 4°C with goat anti cathepsin V
239 (1:400 dilution in PBS with 5% BSA, R&D Systems), and mouse anti heparan sulfate (10E4:
240 1:400 dilution in PBS with 5% BSA, Amsbio, Cambridge, MA, USA). The slides were
241 washed and further incubated with peroxidase-conjugated goat anti-mouse or mouse anti-goat
242 IgG (1:1,000, R&D Systems) for 1 h. Peroxidase activity in tissue sections was visualized as
243 brown color using 3, 3'-diaminobenzidine as a substrate solution. Lung sections were
244 counterstained with Gill's hematoxylin for 1 min, dehydrated, cleared in xylene, and mounted
245 in Vectamount permanent medium (Vector Labs, Peterborough, U.K.)
246 Immunofluorescence (IF) assays on CatV and HS: Non-specific binding sites were blocked
247 with PBS containing 5% BSA and 5% goat serum for 2 h, at room temperature. Sections were
248 then incubated overnight at 4°C with goat anti-CatV (1:100 dilution in PBS containing 5%
249 BSA and 5% goat serum) and mouse anti-HS 10E4 (1:100 dilution in PBS containing 5%

250 BSA and 5% goat serum). Slides were washed and further incubated with fluorescein-labeled
251 anti-mouse IgM antibody (1:2,000, Molecular Probes) or anti-goat IgG NorthernLights™
252 NL637-conjugated antibody (1:2,000, R&D Systems) for 1 h. Lung sections were
253 counterstained with DAPI (4′,6-diamidino-2-phenylindole) for 1 min, and mounted in
254 Vectamount permanent medium (Vector Labs., Peterborough, U.K). Microscopic images
255 were acquired (Carl Zeiss Axio vert A1 inverted microscope, magnification: x200) and
256 processed with the ZEISS microscope software, ZEN 2 Lite blue and repeated three times on
257 three separate tissue sections. The lack of cross reactivity of anti-CatV antibody was checked
258 by western blot analysis on human cathepsins B, K, L, and S (100 ng) as described elsewhere
259 (Sage et al., 2013).
260
261 2.6. Cathepsin V and sulfated GAGs in MPS biological samples- Following running of MPS
262 cell-free supernatants (50 µg of total protein/well; 12% SDS-PAGE under reducing
263 conditions) CatV was immunodetected by a mouse anti CatV primary antibody (1:1,000)
264 incubated overnight at 4°C. Horseradish peroxidase (HRP)-conjugated anti-IgG antibody
265 (1:5,000) was incubated for 1 h at room temperature, and immune-positive bands were
266 visualized using an enhanced chemiluminescence assay kit (ECL Plus Western blotting
267 detection system; Amersham Biosciences, UK). Assays (triplicate) were repeated at least
268 three independent times. In addition, a quantitative analysis of CatV was performed in MPS
269 and non-MPS cell-free supernatants using a sandwich ELISA DuoSet kit (R&D Systems).
270 Sulfated GAGs were quantified with 1,9-dimethylmethylene blue (DMMB, Sigma-Aldrich),
271 (Barbosa et al., 2003). Absorbance was measured at 654 nm (Cary 100 spectrophotometer,
272 Agilent, France) and all values were reported to a final protein content (100 µg). Finally,
273 concentrations of sulfated GAGs were determined by using a calibration curve of similarly
274 treated commercial C4-S solutions (1-10 µg/mL). In parallel, CS, DS and HS content in MPS
275 and non-MPS biological samples were determined by ELISA (AMS Biotechnology,
276 Abingdon, UK) (n=3, triplicate).
277
278 2.7. Titration of cathepsins in MPS and non-MPS lung biological samples- Overall
279 endopeptidase cysteine cathepsin concentration in cell-free supernatants (sputum and tracheal
280 aspirates: 30 µg of total protein) from MPS and non-MPS patients, as reported elsewhere
281 (Naudin et al., 2011). Assays were performed in triplicates and repeated at least three times.
282

283 2.8. Activity of exogenous cathepsin V in the presence of biological samples- The activity of
284 recombinant CatV (0.5 nM) was measured *in vitro* at 37 °C without or with increasing
285 amounts of cell-free supernatants (corresponding to 3-300 ng of total protein) from sputum
286 and tracheal aspirates of MPS patients in 100 mM sodium acetate buffer, pH 5.5, 0.01%
287 Brij35, 10 mM DTT, using Z-Phe-Arg-AMC (20 µM) as a substrate. The activity was
288 measured by spectrofluorometry (λ_{ex}=350 nm, λ_{em}=460 nm). The same experiment was
289 carried out with biological samples pretreated with glycosidases (heparinase I, II, and III,
290 chondroitinase B, and Δ-4,5-glycuronidase) (180 mU/mL), sodium chromate (10 mM), and
291 Dnase I (100 mU/mL) during 48 h at 37°C under vigorous agitation. Controls were performed
292 with non-MPS patients. All kinetic measurements were made in triplicates and repeated three
293 times independently.
294
295
296 2.9. Activity of recombinant cathepsin V in the presence of CHO cell-free lysates- Chinese
297 Hamster Ovary (CHO) cell lines K1 (HS positive, American Type Culture Collection: ATCC,
298 code CCL-61) and 2244 (HS negative, pgsD-677, ATCC code CRL-2244) were a kind gift
299 from Dr. Romain Vivès (Institut de Biologie Structurale, Grenoble, France). CHO cells were
300 cultured at 37°C, under 5% CO2, in EMEM supplemented with 10% fetal calf serum,
301 penicillin (50 IU/mL), and streptomycin (50 µg/mL). CHO cells were harvested at a density
302 of approximately $2x10^6$ cells/mL, centrifuged at 200 *g* for 10 min, then washed once with the
303 preservative buffer (100 mM sodium acetate, pH 5.0, 0.5 mM PMSF, 0.5 mM EDTA, 40 µM
304 pepstatin A, and 1 mM MMTS). The cell pellet was resuspended to achieve a density of
305 approximately $5x10^8$ cells/mL. Cell lines K1 and 2244 disruption was accomplished by
306 syringing the harvested cell pellet through a 20-gauge needle, and CHO cell-free supernatants
307 were recovered after centrifugation (10,000 *g*, 10 min). Protein concentration was determined
308 by a BCA assay, while sulfated GAGs and HS contents were measured using DMMB and
309 ELISA assays, respectively. CatV (1 nM) was incubated with each cell lysate (K1 and 2244,
310 50 µg of total protein) in 100 mM sodium acetate buffer pH 5.5 containing 2 mM DTT. The
311 residual activity was measured after addition of Z-Phe-Arg-AMC (20 µM) (λ_{ex}=350 nm,
312 λ_{em}=460 nm). Assays were repeated under the same conditions using CHO K1 cell-free
313 supernatants pretreated with a solution containing glycosidases (heparinase I, II, and III,
314 chondroitinase B, and Δ-4,5-glycuronidase) (180 mU/mL), sodium chromate (10 mM), and
315 Dnase I (100 mU/mL) for 48 h at 37°C under robust agitation. All kinetic measurements were
316 performed in triplicates and repeated three times.

317

318 2.10. Complex formation between cathepsin V and HS- Recombinant CatV (1 µg) was
319 incubated in the presence or absence of HS (0.15%, w/v, 14 kDa) in a final volume (100 µL)
320 for 10 min in 100 mM sodium acetate buffer, pH 5.5. Samples were then applied to a size
321 exclusion Superdex 200 column (AKTA purifier 900 HPLC system, Amersham,
322 GEHealthcare Bio-Sciences AB, Uppsala, Sweden), previously equilibrated in the same
323 buffer. Protein elution was monitored at 280 nm. The calibration curve was obtained using the
324 standard protein molecular mass markers (Amersham). CatV enzymatic activity was recorded
325 for each fraction (0.5 mL) using Z-Phe-Arg-AMC (20 µM) as substrate. Immunoreactive
326 CatV was detected using a polyclonal goat anti-human CatV antibody (1:1,000) as described
327 previously. HS was revealed in collected fractions using the DMMB assay. Alternatively,
328 dissociation equilibrium constant (K_D) determination between recombinant CatV and HS
329 (0.15%) was measured by surface plasmon resonance imaging (SPRi), as reported elsewhere
330 (Sage et al., 2013).
331

332 2.11. Molecular modeling of interactions between Cathepsin V and HS- Autodock 3 was first
333 used for docking HS, heparin and C4-S tetrasaccharide to CatV (PDB ID: 1FH0) (Morris et
334 al., 1998). The ligands were modeled using GLYCAM06 parameters (Kirschner et al., 2008).
335 The charges of the ligands were previously integrated into the corresponding libraries of GAG
336 monomeric units (Pichert et al., 2012). The protocols for molecular docking and clustering
337 previously optimized for protein-GAG systems were used (Panitz et al., 2016). Structures of
338 CatV/GAG complexes were then used for molecular dynamics (MD) simulations with
339 AMBER 14 (Case et al., 2017). The details for the MD protocols are detailed elsewhere
340 (Panitz et al., 2016). Free energy calculations and per residue decomposition were performed
341 using Molecular Mechanics-Generalized Born Surface Area (MM-GBSA) with gb = 2
342 (Onufriev et al., 2002) implemented in AMBER for 100 frames evenly distributed in the
343 productive MD run. Analysis of the trajectories was done using the cpptraj module of
344 AMBER and VMD for visualization (Humphrey et al., 1996). Alternatively, assays were
345 performed on CatL (PDB ID: 2XU3).
346

347 2.12. Kinetic parameters of wild-type cathepsin V and K20G cathepsin V mutant with GAGs-
348 CatV (0.5 nM) was incubated 10 min in the activity buffer in the presence or absence of HS,
349 C4-S, C6-S, Hep, DS, and HA, respectively (0.15 and 0.3%, w/v) at 37°C. CatV activity was
350 then monitored using Z-Phe-Arg-AMC (20 µM) as a substrate. Experiments with HS were

351 repeated in the presence of increasing amount of NaCl (0-0.5 M). Assays (triplicate) were
352 achieved three times in separate experiments, and relative data are given as means±SD.
353 Steady-state kinetics were assessed as previously described (Sage et al., 2013). Similar assays
354 were repeated with K20G CatV (0.5 nM) and HS (0.15%, w/v).
355 Further, the peptidase activity of CatV was recorded in the presence of increasing amounts of
356 HS (0–0.01%), using Z-Phe-Arg-AMC (1–20 µM) as substrate. Data were plotted using the
357 equation 1/V=f(1/S) (i.e., Lineweaver-Burk plot). Inhibition data were fit by nonlinear
358 regression analysis using the non-competitive model inhibition to determine the equilibrium
359 dissociation constant (K_i) (GraphPad Software). All measurements were performed three
360 times in triplicate.
361
362 2.13. Inhibition of cathepsin V by perlecan and HS derivatives- CatV (0.5 nM) activity was
363 measured in the presence or absence of perlecan (0.1-2 µg/mL), aggrecan (0.1-2 µg/mL), and
364 synthetic HS di- (dp2) and tetra-saccharide (dp4; 0.001-0.005%, w/v) (Liu et al., 2010) in the
365 activity buffer, using Z-Phe-Arg-AMC (20 µM) as a substrate. Control experiment was
366 carried out with perlecan (2 µg/mL) pretreated with heparinase I (2 U/mL) in the activity
367 buffer during 15 minutes at 37°C. Assays were repeated in the presence of Surfen (10 µM).
368 All measurements were performed three times in triplicate.
369
370 2.14. Inhibition of the elastolytic activity of cathepsin V by HS- Elastin-Congo Red conjugate
371 (10 mg/mL) was incubated at 37°C overnight under vigorous agitation with MPS samples (50
372 µg of total protein) in 100 mM sodium acetate buffer, pH 5.5 containing 10 mM DTT, in the
373 presence or absence of Surfen (10 µM). Controls were performed by preincubating previous
374 mixtures with cathepsin inhibitors: E-64 (100 µM), CA-074 (1 µM), CatL inh.7 (1 µM),
375 LHVS (10 nM) and Odanacatib (1 µM). In another set of experiments, aliquots of 10 mg/mL
376 of elastin-Congo Red conjugate were incubated with wild-type CatV (1 µM) or K20G CatV
377 (1 µM) in the presence or absence of HS (0.15 %) in 100 mM sodium acetate buffer, pH 5.5
378 containing 2 mM DTT, and the mixture was vigorously vortexed at 37°C overnight. All
379 assays were stopped by centrifugation (13,500 g, 4°C) to remove the supernatant from the
380 insoluble contents (pellet). The absorbance of the supernatant was measured at 490 nm by
381 spectrophotometry (Cary 100 spectrophotometer, Agilent). All measurements were performed
382 three independent times in triplicate. Similar experiments were repeated under the same
383 conditions with insoluble elastin from bovine neck (10 mg/mL) in the absence and presence
384 of CatV (1 µM) for scanning electron microscopy. Pellets were then fixed by incubation for

385 24 h in 4% paraformaldehyde, 1% glutaraldehyde in 0.1 M phosphate buffer (pH 7.2).
386 Afterwards, samples were then washed in phosphate-buffered saline (PBS), post-fixed by
387 incubation with 2% osmium tetroxide for 1 h, then dehydrated by ethanol and dried in
388 hexamethyldisilazane (HMDS, Sigma-Aldrich). Finally, samples were coated with 40 Å
389 platinum, using a GATAN PECS 682 apparatus (Pleasanton, CA, USA), before observation
390 under a Zeiss Ultra plus FEG-SEM scanning electron microscope (Oberkochen, Germany).
391
392 2.15. Statistical analysis- Data were expressed as mean ± SD unless indicated. Statistical
393 significance between the different values was analyzed by non-parametric Mann-Whitney U
394 test and patients groups comparison were performed with non-parametric Wilcoxon test.
395 Statistical analysis was performed using GraphPad Prism (GraphPad software, San Diego,
396 CA, USA). Differences at a P-value < 0.05 were considered significant.
397
398
399
400
401

402 **3. Results**
403
404 **3.1. Cathepsin V and heparan sulfate colocalize in MPS-I lung biopsy**
405 The expression of CatV in lung tissue from a 2-year old female with MPS-I (Hurler
406 syndrome) was investigated by IHC (**Figure 1**). Main clinical and pathological details have
407 been described previously (Gupta et al., 2013). Briefly, the stained lung tissue sections
408 showed pulmonary parenchyma and bronchial structures modified by autolysis lesions due to
409 the autopsy delay. Malformation or dystrophic arteriolar vascular lesions were observed with
410 edematous and concentric wall fibrosis (Fig. 1A), harboring well-formed granulomas with
411 resorptive multinucleated giant cells (MNGCs) containing few lipid crystals deposits (Fig.
412 1B). Well-formed granulomas were less present in the alveolar walls. Numerous plump
413 alveolar macrophages with vacuolated cytoplasm were identified in alveolar spaces (Fig. 1C),
414 including cases engorged with Periodic Acid Schiff positive material (Fig. 1D, e.g.,
415 glycoprotein, carbohydrate and mucins-like structures). Cells, especially endothelial and
416 bronchial epithelial cells, ubiquitously expressed significant amount of CatV (Fig. 1E, F).
417 Moreover, a fluorescence overlay of CatV and HS probes was observed predominantly in
418 bronchial epithelial cells in MPS-I lung tissue, suggesting a possible co-localization (Fig. 1G).
419
420
421
422
423
424
425
426
427
428
429
430
431
432
433
434
435

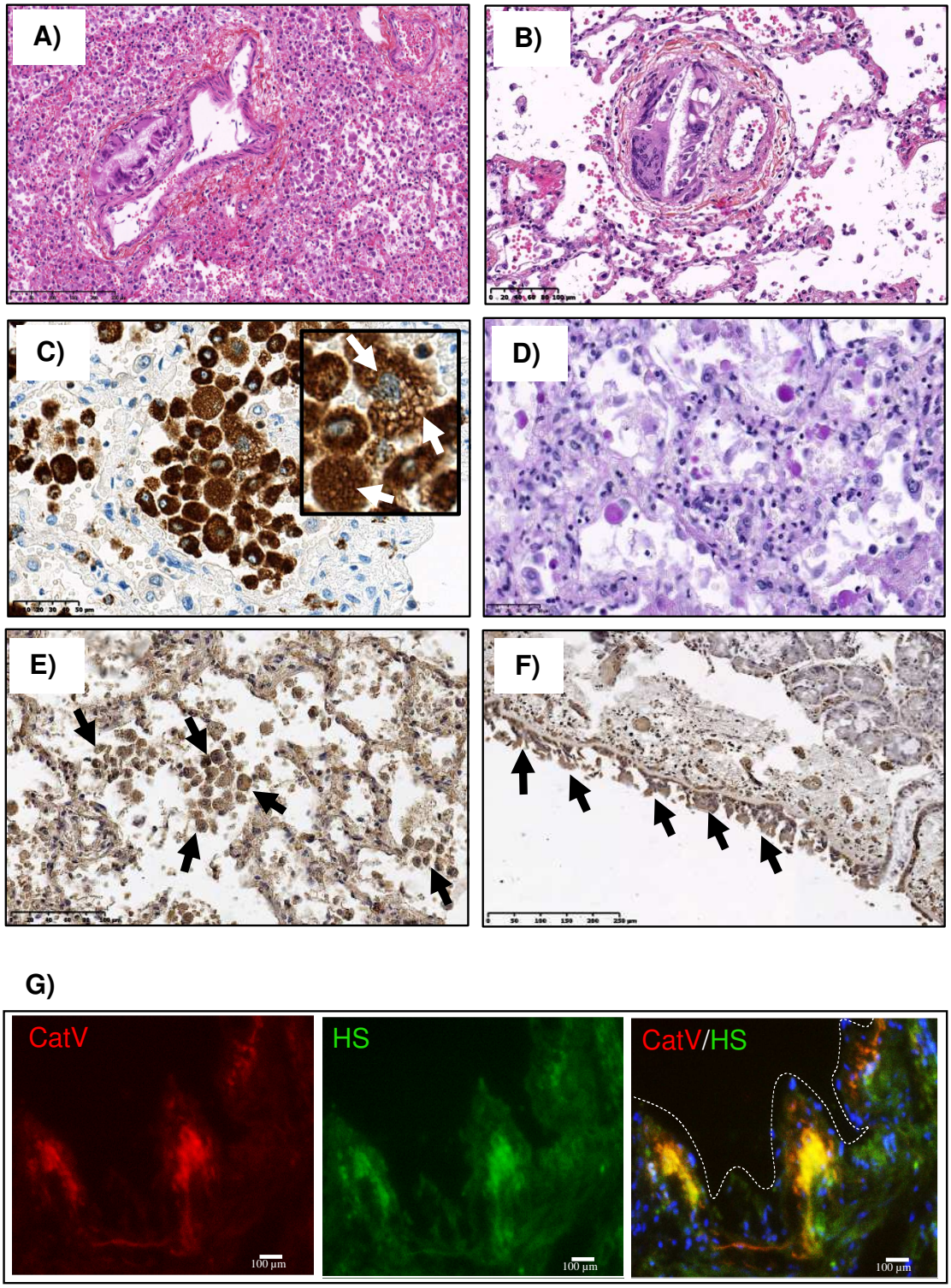

Figure 1: Immunodetection of cathepsin V in MPS-I lung tissue.
Hematoxylin eosin saffron (HES) staining (panels A and B), CD68 IHC (panel C), PAS staining (panel D), CatV IHC (panels E and F), and CatV/HS IF (panel G) were performed on lung tissue obtained from a post-mortem 2-year-old female with MPS-I. A) Mild concentric edematous fibrosis of blood vessels (x10). B) Granuloma exhibiting multinucleated giant cells in venular walls (x20). C) Alveolar macrophages with numerous vacuoles (white arrows) in the cytoplasm (inset) (x40). D) Eosinophils and mucopolysaccharides deposits mainly in alveolar macrophages (x40). E) CatV in

alveolar macrophages (x300) and F) in bronchial cells (x150), as indicated by black arrows. G) Representative IF images (of two independent experiments performed) showing CatV stained in red and HS in green. Merged panel revealed the co-localization of both antigens in bronchial cells. Cell nuclei were stained in blue (DAPI staining). Scale bar is 50 µm (panels C, D), 100 µm (panels B, E, G), and 250 µm (panels A, F).

3.2. Cathepsin V and heparan sulfate levels in MPS-I, II, and III respiratory samples

Given the scarcity of lung biopsies from young MPS patients, we decided to use as biological specimen sputum and tracheal aspirates. Eleven MPS patients with a history of respiratory complaints, and nine non-MPS patients with no respiratory symptoms were recruited. MPS patient characteristics were summarized in **Table 1**. There were more males, which reflects the disease population (in particular MPS-II, an X-linked disease affecting mainly males). The mean age, size and weight of the MPS patients (10± 6 years; 112.3±18 cm; 26.5±11 kg) were not statistically different than control groups (9±6 years; 133±41; 34±22 kg).

Table I: Clinical characteristics of MPS patients.

#	Age (yr)	Sex	Weight (kg)	Height (cm)	Diagnosis (MPS type, subtype)	Enzyme deficiency	Treat-ment	GRSS score
1	11	M	22.3	104	Hurler (I)	IDUA	ERT	4
2	14	F	24.8	106	Hurler (I)	"	ERT	4
3	2	M	14.4	85	Hunter (II)	IDS	ERT	2
4	8	M	49.5	125	Hunter (II)	"	ERT	3
5	4	M	20.5	105	Hunter (II)	"	ERT	2
6	2	M	14.1	90	Hunter (II)	"	ERT	2
7	19	M	22.9	114	Hunter (II)	"	ERT	4
8	7	M	29.4	118	San Filippo (III, A)	HNS	no	3
9	18	F	33.4	127	San Filippo (III, B)	NAG	no	2
10	15	M	40.0	149	San Filippo (III, B)	"	no	4
11	6	M	20.8	112	San Filippo (III, C)	HGSNAT	no	1

IDUA: α-L-iduronidase; IDS: iduronate-2-sulfatase; HNS: heparan-N-sulfatase; NAG: N-acetyl-glucosaminidase; HGSNAT: heparan α-glucosaminide-N-acetyltransferase; ERT: enzyme replacement therapy; no: no specific treatment. MPS patients were assigned with a number (#).
The global respiratory symptoms severity (GRSS) score was assessed for each patient on the basis of four sub-type evaluations: ear-nose-throat symptoms (chronic rhinitis or sinusitis, otitis, adeno-tonsillar hypertrophy, hearing loss, macroglossia, stridor), pulmonary symptoms (dyspnea, wheezing, cough, sputum, asthma, bronchitis, pneumonia), clinical symptoms of obstructive sleep apnea, and skeletal abnormalities causing restrictive lung disease (scoliosis, kyphosis, ribcage narrowing, chest wall deformity). The GRSS was graduated from 0 to 4, corresponding to the number of sub-types symptoms reported for each patient.

The expression levels of CatV in cell-free supernatants of induced sputum and tracheal aspirates of MPS patients was evaluated by Western-blot and ELISA (**Figure 2**). Both pro-CatV (as full or partially processed proforms) and mature CatV were detected by Western blots analysis (Fig. 2A). We did not find a significant difference in expression level of immunoreactive CatV (ELISA assay) between MPS patients and non-MPS patients (379±181 pg/mL *vs.* 439±256 pg/mL, normalized to total homogenate protein content of 100 µg in each sample) (Fig. 2B). Also, there was no difference in CatV levels between MPS types (*supplementary Fig. 1A*). Conversely, ELISA analysis demonstrated that all MPS patients displayed a 4-fold increase of HS levels (19.3±10 ng/mL) compared to controls (3.9±4 ng/mL) ($P<0.0001$) (Fig. 2C). Nevertheless, no significant difference of HS levels was observed between MPS types (*supplementary Fig. 1B*). DS levels were lower (5±8 ng/mL) than HS in MPS patients, but higher compared to controls (1±1 ng/mL) ($P<0.05$, Fig. 2D). No significant difference was observed for chondroitin sulfate (CS) between MPS and non-MPS patients (*supplementary Fig. 1C*). Present data suggest that, among major lung sulfated GAGs, HS concentration is increased substantially in respiratory samples from MPS types I, II, and III. Of note, a significant increase of total sulfated GAGs content (DMMB test) was measured in MPS patients *vs.* controls ($P<0.0001$) (*supplementary Fig. 1D*). Nevertheless, the total sulfated GAGs levels (µg/mL) was higher than HS, DS, and CS levels (pg/mL), this difference probably depending on the presence of other sulfated GAGs, proteoglycans or DNA fragments, which may interact with DMMB as reported by Barbosa et al. (Barbosa et al., 2003). We expanded our observations by comparing HS levels in respiratory samples from the cohort of MPS patients on the basis of the global respiratory symptoms severity (GRSS) (Fig. 2E). Interestingly, the GRSS scores correlated positively ($r_s=0.91$, $P<0.0001$) with HS concentration, suggesting that an elevated HS level is associated with the onset of respiratory-related disorders. In addition, the GRSS scores correlated positively with the age of MPS patients ($r_s=0.6515$, $P<0.0354$, *supplementary Fig 1.E*), supporting that accumulation of GAGs leads to diverse clinical manifestations including respiratory problems that worsen with age.

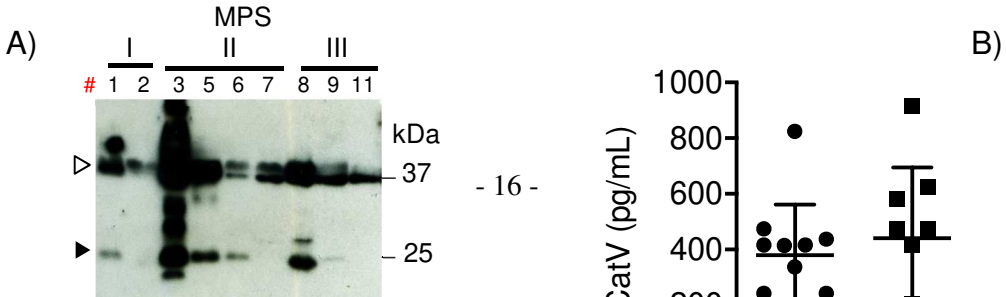

549
550
551
552
553
554
555
556
557
558
559
560
561
562
563
564
565
566
567
568
569
570
571
572

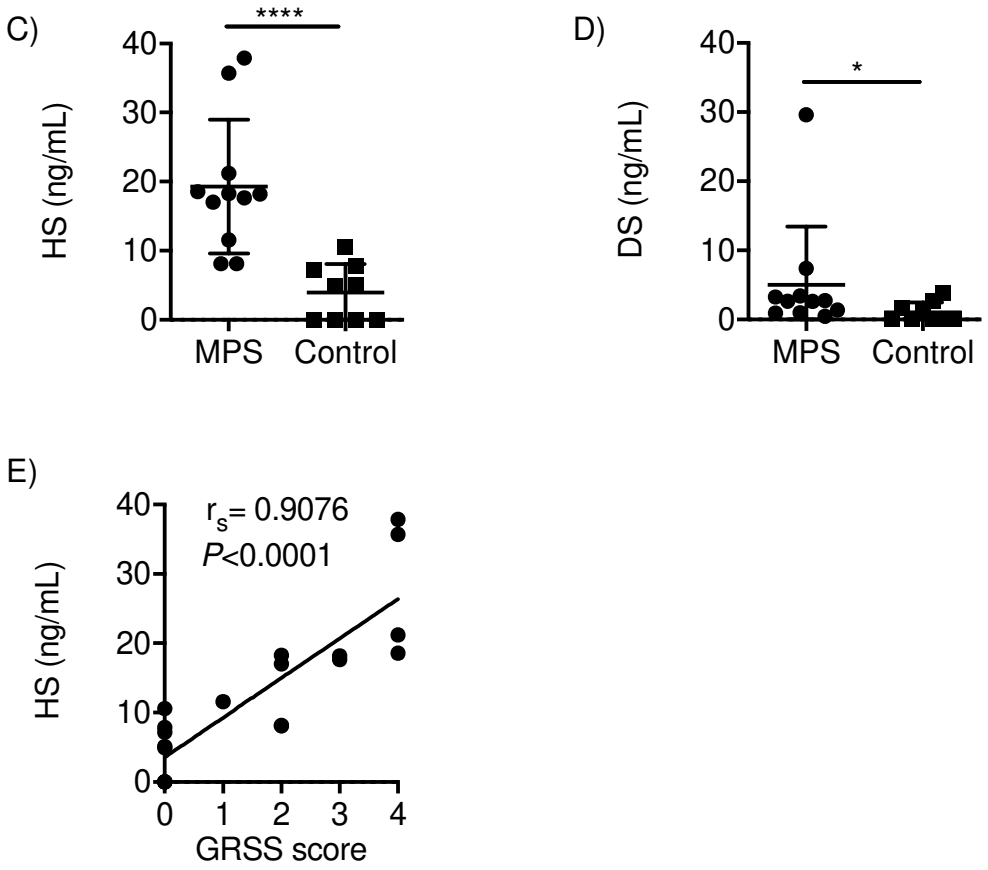

573 **Figure 2: Cathepsin V and heparan sulfate levels in respiratory secretions from MPS-I,**
574 **II, and III patients.**
575 A) Representative western blot (of two independent experiments) reflecting CatV protein expression
576 (white and black arrows: pro- and mature form, respectively) in cell-free supernatants from MPS-I, II,
577 and III respiratory secretions (total protein deposited: 50 µg/well). Number (#) assigned to each MPS
578 patient refers to Table 1. Two MPS (type II and IIIB) samples were not shown due to their limited
579 availability for western blot. B) ELISA protein levels of CatV in MPS (N=11) and non-MPS patients
580 (control, N=9). C) HS concentration determined by ELISA. D) DS concentration determined by
581 ELISA. E) Correlation between HS levels and global respiratory symptoms severity (GRSS) score.
582 The GRSS score was graduated from 0 to 4, corresponding to the number of major clinical respiratory
583 signs/symptoms diagnosed for each patient. Study was completed by linear regression. Spearman
584 coefficient (r_s) and level of significance (*P*) were reported. Statistical analyses were performed using

585 Mann-Whitney *U* test, (**: $P<0.01$; ****: $P<0.0001$). Results are expressed as mean±standard
586 deviation (SD) of three independent experiments.
587

588 **3.3. Cathepsin V activity in MPS-I, II, and III samples**

589 A former report showed that elevated HS concentrations impair CatV activity *in vitro* (Yasuda
590 et al., 2004). Accordingly, we evaluated the ability of HS-enriched MPS samples to inhibit
591 CatV (**Figure 3**). We first measured the total endopeptidase activity of cysteine cathepsins in
592 cell-free supernatant from both MPS and non-MPS samples, using Z-Phe-Arg-AMC as a
593 broad-spectrum substrate, and E-64 as titration reagent. A ~2.5-fold decrease of active
594 cathepsins was measured in all MPS types (259±74 nM) compared with controls (616±296
595 nM) (Fig. 3A; $P<0.05$). Also, this drop of active forms of cathepsins correlated negatively
596 (Fig. 3B; $r_s=-0.66$; $P=0.0015$) with HS levels and sulfated GAG content ($r_s=-0.79$; $P<0.0001$,
597 *supplementary Fig. 1F*), and with the GRSS scores (Fig. 3C; $r_s=-0.7052$; $P=0.0005$). Due to a
598 lack of both selective substrate and inhibitor of CatV, an indirect method was devised to
599 uncover the influence of GAG on CatV activity. Three serial dilutions of cell-free
600 supernatants (corresponding to 300, 30, and 3 ng of total protein, respectively) were mixed
601 with a constant amount of exogenous recombinant CatV (0.5 nM), before monitoring the
602 residual activity by Z-Phe-Arg-AMC (Fig. 3D-G).
603
604
605
606
607
608
609
610
611
612
613
614
615
616
617
618

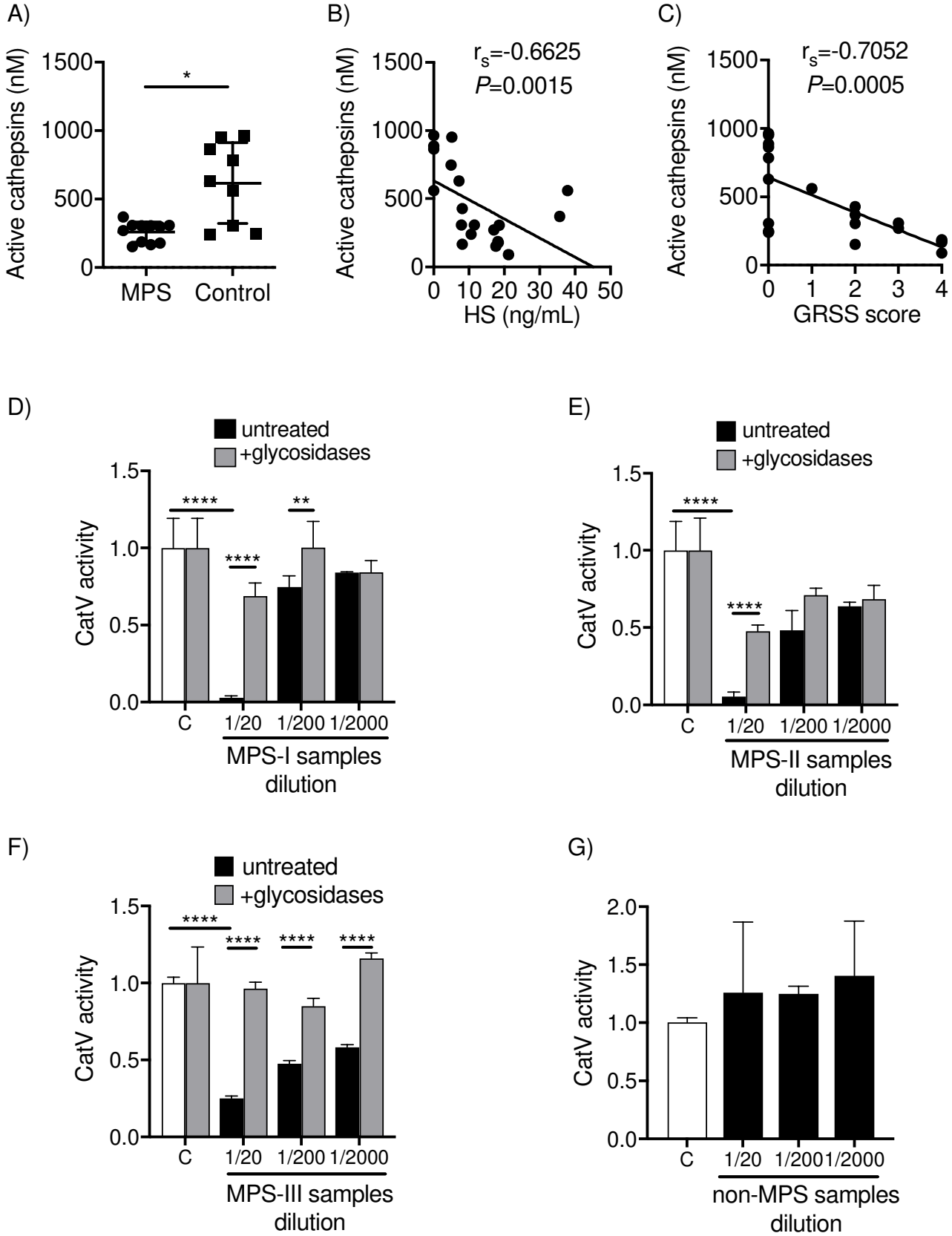

Figure 3: Inhibition of cathepsin V in respiratory secretions from MPS-I, II, and III patients.

660 A) Active cathepsins concentration was determined by E-64 titration (MPS and non-MPS samples; 30
661 µg of total protein). B) Correlation between concentrations of active cysteine cathepsins and HS level.
662 C) Correlation between concentrations of active cysteine cathepsins and GRSS score. D) Recombinant
663 CatV (0.5 nM) was incubated for 10 min in the activity buffer alone (control: C) or with different
664 dilutions of cell-free supernatants from individual respiratory secretion of MPS-I (N=2), E) MPS-II
665 (N=5), F) MPS-III (N=4), and G) non-MPS (N=9). The same experiment was carried out with samples
666 pre-treated with glycosidases (heparinases I, II, III, and Δ-4, 5-glycuronidase). Residual activity
667 (tripicate) was measured with Z-Phe-Arg-AMC (20 µM). The relative activity was determined based
668 on the residual protease activity of CatV after incubation (control). Results are expressed as mean±SD
669 of three independent experiments. Statistical analyses were performed using Mann-Whitney *U* test
670 (**: $P<0.01$; ***: $P<0.001$; ****: $P<0.0001$).
671
672 No endogenous peptidase activity toward Z-Phe-Arg-AMC was detected in the diluted
673 samples prior addition of exogenous CatV. CatV activity was significantly reduced in 1:20
674 dilution samples of all MPS types ($P<0.0001$) and rose progressively along the increasing
675 serial dilutions (Fig. 3D-F). In contrast, no significant difference in the activity of CatV was
676 detectable in non-MPS individuals (Fig. 3G). Pre-treatment of MPS samples with
677 glycosidases (heparinase I, II, and III, chondroitinase B and Δ-4,5-glycuronidase) yielded to a
678 significant retrieval of CatV activity in the presence of MPS-I (Fig. 3D) and MPS-II samples
679 (Fig. 3E). CatV activity was fully recovered in the presence of MPS-III samples (Fig. 3F).
680 Taken together, present results support that accumulation of GAG, including HS, could
681 potently impair lung CatV activity during MPS.
682
683 **3.4. Inhibition of cathepsin V by heparan sulfate**
684 Cell-free lysates from wild-type CHO (HS positive strain) and HS-deficient CHO (HS
685 negative strain) cultures were incubated with recombinant CatV (**Figure 4**). A striking
686 difference was observed between HS positive and HS negative CHO samples, since WT
687 lysates but not HS deficient lysates, impaired peptidase CatV activity ($P<0.0001$) (Fig. 4A).
688 Conversely, CatV activity was fully recovered when HS positive CHO lysates were treated
689 beforehand with heparinases I, II, III, and Δ-4,5-glycuronidase ($P<0.001$), and thus confirmed
690 that HS is a potent inhibitor of CatV. Moreover, this finding was supported by testing various
691 GAGs at concentrations that mimic those found in liver, lungs and ovaries in MPS models
692 (Chung et al., 2007; Haskins et al., 1992). Indeed, among GAGs tested, only HS and DS
693 reduced significantly, in a dose dependent manner the peptidase activity of CatV ($P<0.05$)
694 (Fig. 4B). HS (0.15%) produced a ~5-fold drop of the specificity constant (k_{cat}/K_m), which
695 mostly affected the catalytic activity of CatV (decrease of the k_{cat} value) (**Table 2**). Increase
696 of the ionic strength by addition of NaCl restored CatV peptidase activity in a dose-dependent

manner, suggesting that electrostatic interactions mainly governed binding of CatV to negatively charged HS (Fig. 4C). We next investigated the mechanism of inhibition of CatV by HS. HS inhibited peptidase CatV activity according to a non-competitive inhibition mechanism (K_i estimated = 11.4±3 μM) (Fig. 4D). Then, we incubated CatV with insoluble Congo Red Elastin to determine whether HS could also alter the proteolytic activity of CatV. Figure 4E revealed that HS (0.15%) compromised the elastolytic activity of CatV (90±2% inhibition, $P<0.001$). This was further corroborated by SEM analysis. While long elastin fibers (from bovine neck) were broken up into shorter fibrils by CatV, presence of HS impaired fragmentation of elastin fibers (Fig. 4F).

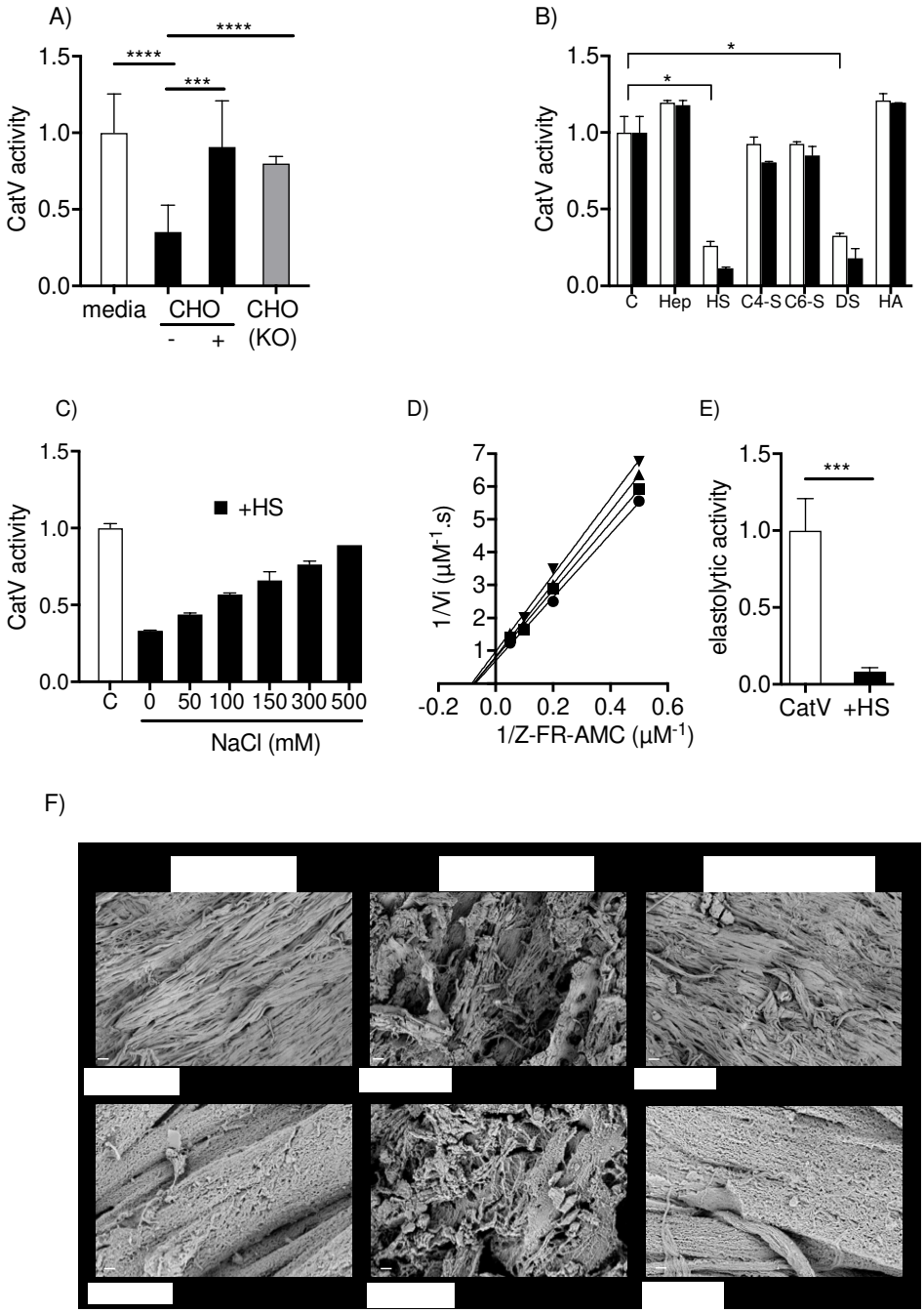

Figure 4: Inhibition of cathepsin V by heparan sulfate.

A) Recombinant CatV (0.5 nM) was incubated for 10 min in the activity buffer with cell culture media alone (control), CHO cells lysate (-), CHO cell lysate pre-treated with glycosidases (+), and CHO cells lysate lacking HS (KO). B) CatV (0.5 nM) was incubated in the absence (control: C) or in the presence of different GAGs (Hep: low molecular weight heparin; HS: heparan sulfate; C4-S/C6-S: chondroitin 4/6-sulfate; DS: dermatan sulfate; HA: hyaluronic acid) at 0.15% (weight/volume, w/v) (white bar) and 0.3% (black bar) in the activity buffer. C) CatV (0.5 nM) activity in the presence of HS (0.1%) is restored by NaCl. Hydrolysis of Z-Phe-Arg-AMC (20 µM) was monitored with a spectrofluorometer. The mean values±SD of three triplicate independent assays are expressed as relative value for the

767 hydrolysis of Z-Phe-Arg-AMC in each sample (normalized to control=1). D) Lineweaver-Burk plot
768 analysis of CatV (0.5 nM) velocity (Vi) with varying Z-Phe-Arg-AMC concentrations (1-20 µM) at a
769 HS concentration of 0-0.01% (0 % : ● , 0.001 % : ■, 0.005% : ▲, 0.01% : ▼). E) Elastolytic activity
770 of CatV (1 µM) in the absence (white bar) or presence of HS (0.15%, black bar) was measured by the
771 insoluble Congo Red elastin (10 mg/mL) spectrophotometry assay and was expressed as relative value
772 (normalized to control=1) at 490 nm. F) Representative electron micrographs (SEM) showing the
773 effect of HS (0.3%) on CatV (1 µM) elastolytic activity toward bovine neck elastin powder (10
774 mg/mL) after overnight incubation. Magnification bars, 10 µm (upper panel) and 1 µm (lower panel).
775 Results were analyzed using Mann-Whitney U test (*P*-value *: $P<0.05$; ***: $P<0.001$; ****:
776 $P<0.0001$).
777
778
779 **Table 2:** Kinetic parameters for the hydrolysis of Z-Phe-Arg-AMC by CatV in the presence

GAG (0.15%)	Sulfatation degree (number of SO_4^{2-} by disaccharide)	[Disaccharide]n	k_{cat} (s^{-1})	K_m (µM)	k_{cat}/K_m ($x10^6 M^{-1}.s^{-1}$)
-	-	-	7.6±0.5	6.9±1.6	11.0±0.9
+ Hep	2.5	L-IdoA2S-α(1→4)-D-GlcNS6S-α(1→4)	5.3±0.3	5.7±1.7	9.0±1.0
+ HS	0.8	D-GlcA-β(1→4)-D-GlcNAc-α(1→4)	1.4±0.2	5.7±1.0	2.4±0.6
+ C4-S	0.9	D-GlcA-β(1→3)-D-GalNAc4S-β(1→4)	5.4±0.2	4.5±0.6	12.0±1.1
+ C6-S	0.9	D-GlcA-β(1→3)-D-GalNAc6S-β(1→4)	8.2±0.9	6.9±1.2	11.8±0.9
+ DS	1.1	L-IdoA-α(1→3)-D-GalNAc4S-β(1→4)	1.3±0.2	4.8±1.2	2.7±0.1

780 of GAGs
781
782
783 **3.5. Binding of heparan sulfate to cathepsin V**
784 CatV (25 kDa) and HS (14 kDa) were eluted at 19.5 mL and at >25 mL, respectively (size
785 exclusion chromatography, Superdex 200 column). Analysis of a mixture of CatV and HS
786 revealed the presence of an additional peak at 200-250 kDa (elution volume: 5-8 mL), which
787 was specifically detected by DMMB assay (**Figure 5A**). Also, peptidase CatV activity was
788 detected in both 25 kDa and 200-250 kDa peaks, endorsing that HS bound to CatV in
789 solution. The binding affinity between HS and CatV was calculated by surface plasmon
790 resonance imaging (Fig. 5B). The dissociation equilibrium constant value (K_D) of the
791 HS/CatV complex was 55±5 nM. This high affinity binding value was in accordance with
792 previous finding above. Molecular modeling studies were further performed to tentatively
793 understand the basis of CatV inhibition and identify putative HS binding sites on CatV (Fig.
794 5C). According to HS chains vary widely in extent in epimerization and sulfation, we
795 conducted computational experiments using two well-defined HS tetrasaccharide models: a

796 highly sulfated variant corresponding to Hep, which has α-L-iduronic acid-2-sulfate-*N*-sulfo-
797 α-D-glucosamine-6-sulfate (IdoA2S-GlcNS6S) disaccharide units and an unsulfated variant
798 with β-D-glucuronic acid-*N*-acetyl-*a*-D-glucosamine (GlcA-GlcNAc) disaccharide unit.
799 Docking scores were obtained for tetrasaccharides as the smallest unit required for specific
800 protein-GAG interactions based on the data available in the PDB (Samsonov & Pisabarro,
801 2016). Among the 50 top scoring complexes obtained, two major binding sites of unsulfated
802 HS variant were identified on CatV. The most populated cluster (21 poses) was located within
803 the active site cleft (Q19, K20, Q21, G23, S24, C25, N66, G67, and W190) while the second
804 one (15 poses) (V169, G170, Y171, G172, K182, Y183, W184, L185, V186, V200, K201,
805 and I202) located on the backside of the enzyme, away from the catalytic cleft. By contrast,
806 no clusters of Hep were observed in the catalytic domain of CatV (*supplementary Figure 2A*).
807 Heparin formed multiple contacts with CatV residues scattered on the backside of the
808 molecule, in the vicinity to the second binding site of unsulfated HS. Furthermore, no binding
809 poses of C4-S tetrasaccharide (β-D-GlcA-N-acetyl–β-D-galactosamine-4-sulfate (GalNAc4S)
810 disaccharide units) were predicted in the active site of CatV (supplementary Fig. 2B),
811 suggesting that unsulfated HS accommodated preferentially the active cleft of the enzyme.
812 These results corroborated the difference in the inhibition of CatV peptidase activity
813 measured by HS, Hep, and C4-S, as previously reported.
814
815
816
817
818
819
820
821
822
823
824
825
826
827
828

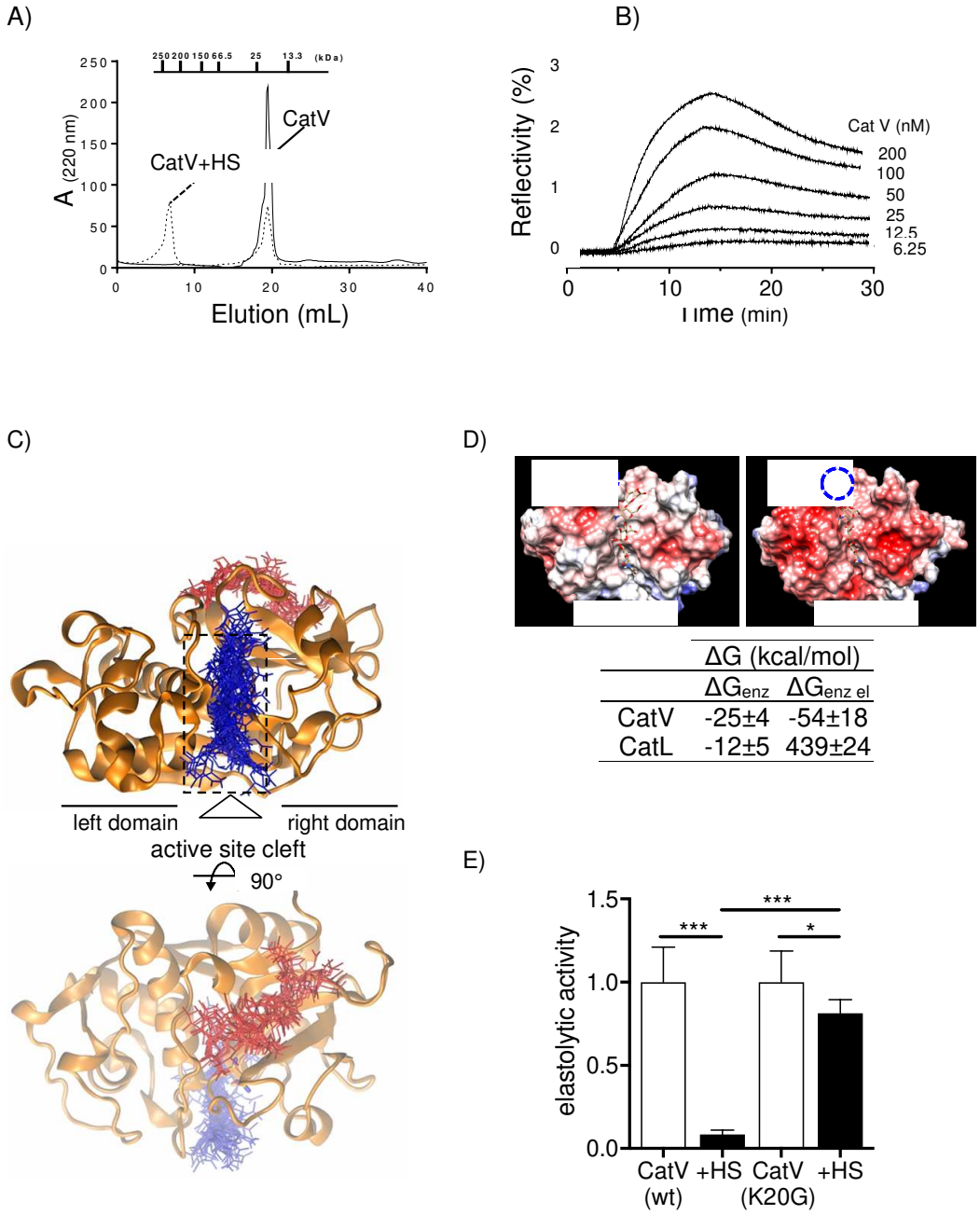

Figure 5: Binding of heparan sulfate to cathepsin V.

A) Size-exclusion chromatography profiles of CatV in the absence (solid line) or presence of HS (dashed line). The elution volumes of size standards under identical conditions are shown above the graph. B) CatV-HS binding analyzed by surface plasmon resonance imaging. Compiled sensorgrams of the kinetics of the interactions between CatV (6.25–200 nM) with HS-bearing biochips. C) Clusters from 50 top-scored docking solutions of tetrameric HS (unsulfated) binding to CatV. A "top view" of CatV and "back view" following a 90° rotation around the horizontal axis is shown. The most populated cluster (blue) is located within the active cleft of the enzyme, while the second major cluster (red) is on the backside. D) Docking of tetrameric unsulfated HS within the active site of CatV

865 (PDB:1FH0) and CatL (PDB:3HHA). MD-based free energy calculations (ΔG) for the obtained
866 binding poses of unsulfated HS were evaluated in the active site (ΔG_{enz}), outside the active site
867 (ΔG_{out}). Electrostatic component of binding energy was reported ($\Delta G_{enz\ el}$) ($\Delta G_{out\ el}$). Surface
868 electrostatic potential of both enzymes is shown. Blue areas correspond to positive charge and red
869 areas to negative charge. Among residues of the active cleft of CatV that are predicted to interact with
870 structural model of HS, K20 was a target residue for mutation to generate a cathepsin L-like mutant,
871 K20G, of CatV. K20 and G20 residues location is depicted by a circle. E) A bar chart analysis
872 showing the effect of HS (0.15%, black bar) on the elastolytic activity (Congo Red elastin assay) of
873 K20G CatV mutant compared with wild-type CatV. Results were analyzed using Mann-Whitney U
874 test (*P*-value *: $P<0.05$; ***: $P<0.001$).
875

876 **3.6. Lys20 is an essential residue within the active-site cleft of cathepsin V for interaction**
877 **with HS**

878 Human CatV and CatL that share 78% identity and 85% homology of protein sequences
879 display similar three-dimensional structures (Fig. 5D). Although both enzymes disclose
880 similar subsite specificities (Choe et al., 2006), high concentration (0.15%) of cartilage and
881 bone-resident GAGs did not inhibit CatL peptidase activity (Li et al., 2000). Docking and MD
882 analysis of unsulfated HS tetrasaccharide on the active site of CatL revealed striking
883 differences with CatV (Fig. 5D). Binding free energy (ΔG_{enz}) calculated by MM-GBSA
884 approach was about twice less favorable for CatL compared to CatV. In addition, electrostatic
885 potential surface of residues bordering the active site of CatL is highly negative, thus less
886 energetically favorable to bind to unsulfated HS ($\Delta G_{enz\ el}$=439±24 kcal/mol) compared to
887 CatV ($\Delta G_{enz\ el}$=-54±18 kcal/mol).
888 Next, we analyzed the residues in the CatV cleft that can theorically interact with unsulfated
889 HS and were different than their counterpart in CatL sequence. The only noticeable difference
890 between CatV and CatL was observed at the position 20 within the active-site cleft. CatV
891 possesses a positively charged lysine residue at position 20, which is replaced by a glycine
892 residue in CatL. Hence, we generated and expressed in *P. pastoris* a K20G CatV mutant.
893 Specificity constant values for Z-Phe-Arg-AMC hydrolysis by wild-type CatV
894 (k_{cat}/K_m=11±0.9x10^6 M^{-1}) and by K20G CatV mutant (k_{cat}/K_m=8.3±1x10^6 $M^{-1}.s^{-1}$) were
895 comparable. This indicates that the overall peptidase activity of the CatV mutant was not
896 affected by this single mutation. Contrary to CatV, addition of HS (0.15%) did not change
897 significantly the specificity constant of K20G CatV mutant (k_{cat}/K_m=9.63±1x10^6 $M^{-1}.s^{-1}$).
898 Although a slight but significant impairment of the elastolytic activity of K20G CatV mutant
899 was observed in the presence of HS ($P<0.05$), K20G CatV still retained a greater elastolytic
900 activity than HS-bound wild-type CatV (P=0.0006) toward Congo Red Elastin (Fig. 4E). This

901 result supported that positively charged Lys20 played a critical role in the binding of HS chain
902 within the active site-cleft of CatV.
903
904 **3.7. Surfen is a potent antagonist of cathepsin V inhibition by HS and HS-related**
905 **glycosaminoglycans**
906 In MPS, abnormal levels of heparan sulfate proteoglycans (HSPGs) and accumulation of HS
907 chains (both native or partially degraded forms) are found (De Pasquale & Pavone, 2019; Pan
908 et al., 2005). To address the biological significance of HS attached to a core protein and HS
909 fragments in the inhibition of CatV, the effect of perlecan (a.k.a. heparan sulfate proteoglycan
910 2) and synthetic HS di- and tetra-saccharides were examined. Perlecan inhibited CatV in a
911 concentration-dependent manner (**Figure 6A**), with 80±5% inhibition at a concentration of 2
912 μg/mL, contrary to aggrecan, a KS/CS-containing proteoglycan (Fig. 6B). To ensure that the
913 observed inhibition was mediated by HS, perlecan was treated with heparinase I. Cleavage of
914 HS chains in perlecan (2 μg/mL) fully restored the peptidase activity of CatV (P<0.0001)
915 (Fig. 6A). Similarly, a consistent decrease in CatV activity was observed with di- and tetra-
916 saccharides of HS (dp2 and dp4, dp: degree of polymerization) (Fig. 6C). Equal percentage
917 (0.001-0.005%, m/v) was used to allow direct comparison between dp2 and dp4. Our results
918 showed that dp4 was significantly more effective than dp2, suggesting that the tetrasaccharide
919 with the repeating unit of *N*-acetyl-α-D-glucosamine/β-D-glucuronic acid (GlcNAc-GlcA)
920 was the minimal length required to inhibit CatV, which was in agreement with *in silico*
921 studies.
922 Several HS competitors/antagonists were reported to regulate the expression and/or reduce
923 binding of HS. Of particular interest is Surfen (bis-2-methyl-4-amino-quinolyl-6-carbamide,
924 *supplementary Figure 3A*), a chemical compound that binds tightly to HS and was reported to
925 antagonize HS-protein interactions (Schuksz et al., 2008). Therefore, we first investigated the
926 effect of Surfen on the inhibition of CatV *in vitro* by HS and derivatives. We chose
927 concentration of HS, perlecan and dp4 eliciting ~50% inhibition of CatV activity using Z-
928 Phe-Arg-AMC as a substrate. First, we checked that Surfen, which exhibits weak fluorescence
929 (λ_{ex}=350 nm, λ_{em}=460 nm) in neutral solution (Schuksz et al., 2008), did not overlap with the
930 fluorescence signal of 7-amido-4-methylcoumarin (AMC) group (*supplementary Fig. 3B*).
931 Addition of Surfen (10 μM) was sufficient to abolish completely the inhibition of CatV by HS
932 (Fig. 6D), HS-containing proteoglycan perlecan (Fig. 6E), and HS dp4 (Fig. 6F).
933
934

935
936
937
938
939
940
941
942
943
944
945
946
947
948
949
950
951
952
953
954
955
956
957
958
959
960
961
962
963
964
965
966

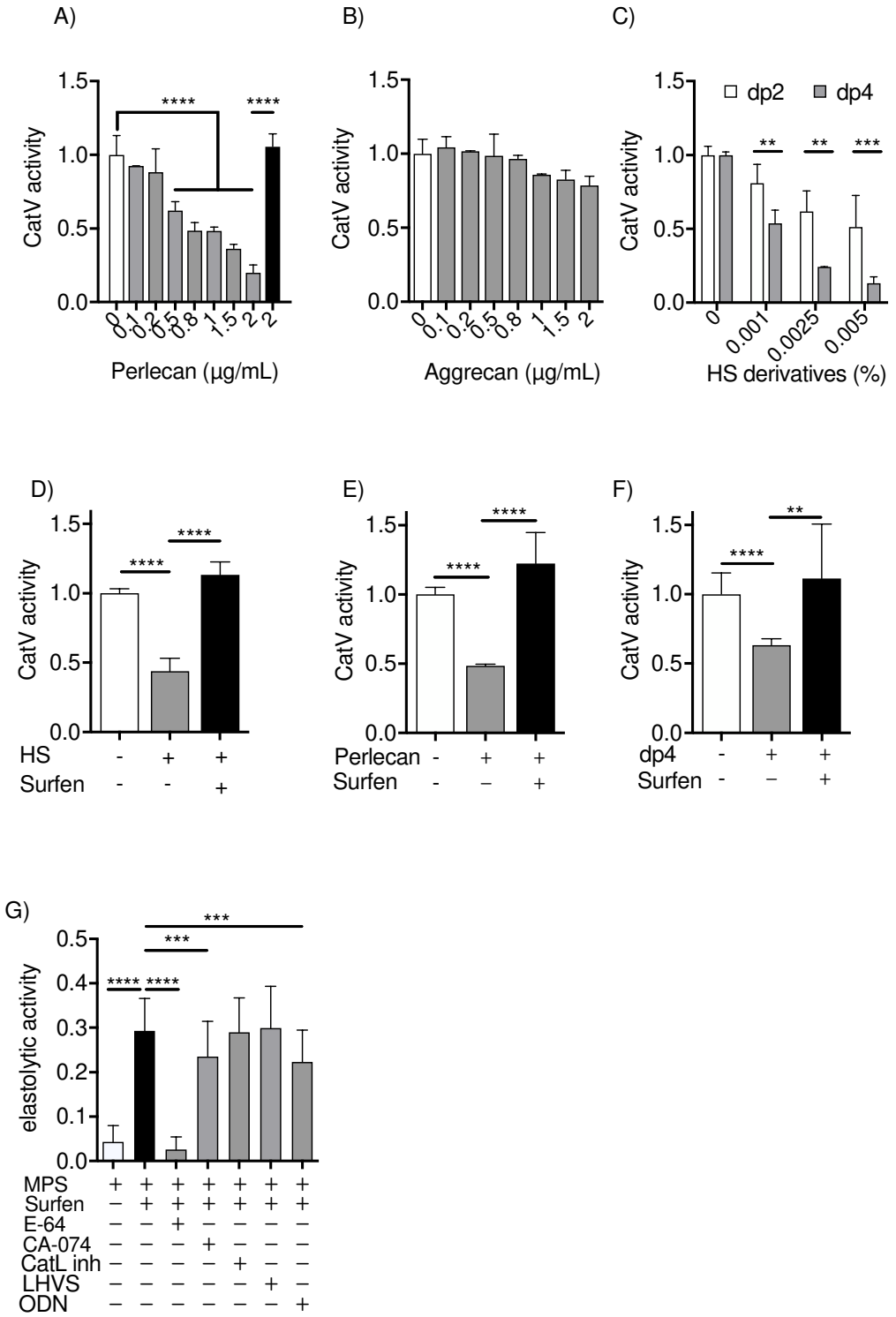

967 **Figure 6: Inhibition of cathepsin V with HS-like derivatives and influence of Surfen**.

968 A) CatV (0.5 nM) was incubated for 10 min the activity buffer in the absence (control) or in the
969 presence of increasing concentrations of perlecan (0-2 µg/mL). Assays were also performed with
970 heparinase I-treated perlecan (2 µg/mL, black bar). B) Effect of aggrecan (0-2 µg/mL) and C)
971 synthetic di- and tetrameric heparan sulfate derivative (dp2, dp4; 0.001-0.005%, m/v) on CatV
972 activity. Residual activity was measured with fluorogenic substrate Z-Phe-Arg-AMC (20 µM) and
973 expressed as relative value (normalized to control=1). D-F) CatV (0.5 nM) was previously incubated
974 in the activity buffer for 10 min with HS from bovine kidney (0.05%) or perlecan (2000 ng/mL) or
975 dp4 (0.01%) before adding Surfen (10 µM). Residual activity was measured with the fluorogenic
976 substrate Z-Phe-Arg-AMC (20 µM). G) Surfen enhanced cysteine cathepsins-mediated elastin
977 degradation in cell-free supernatants from MPS-I, II, and III respiratory secretions. Assays were
978 performed with Congo Red elastin (10 mg/mL) incubated overnight under agitation with individual
979 MPS sample (total protein = 30 µg) in the absence and presence of Surfen (10 µM) in the activity
980 buffer at 37°C. Controls were performed by adding different cathepsin inhibitors : E-64 (100 µM),
981 CA-074 (1 µM), CatL inhibitor (1 µM), LHVS (10 nM) and ODN (1 µM) in the activity buffer at
982 37°C. Results were expressed as mean±SD and were analyzed with GraphPad Prism software using
983 Mann-Whitney test, *P*-value **: $P<0.01$; ***: $P<0.001$; ****: $P<0.0001$.
984
985 We next assessed the effect of Surfen on endogenous cathepsins-mediated elastolytic activity
986 in MPS samples, using Congo Red assays. Interestingly, pretreatment of soluble cell-free
987 supernatants of respiratory secretions with Surfen induced a significant ~6-fold increase of the
988 elastolytic activity compared to untreated MPS samples (MPS-I, II, III specimens) (Fig. 6G).
989 E-64, the broad-spectrum inhibitor of cysteine cathepsins, fully impaired elastolytic activity
990 ($P<0.0001$), while both odanacatib (ODN), a nitrile-based inhibitor of CatK and CA-074, a
991 selective CatB inhibitor led to a moderate but significant reduction of 23% and 20%,
992 respectively. Results endorsed that the elastin degrading activity of MPS samples depends on
993 cysteine cathepsins. Conversely, LHVS, a selective CatS inhibitor, and CatL inhibitor (*N*-(4-
994 biphenylacetyl)-*S*-methylcysteine-(D)-Arg-Phe-β-phenethylamide) did not impair
995 elastinolysis, supporting that the elastolytic activity measured in MPS samples was mainly
996 credited to CatV-related activity.
997
998 **4. Discussion**
999 Respiratory complications (i.e. upper and lower airway obstruction and restrictive pulmonary
1000 disease) are typical irreversible features that affect early MPS patients and contribute often
1001 with cardiovascular abnormalities to death or disability associated with disease evolution.
1002 Current treatments such as hematopoietic stem cell transplantation (HSCT) or enzyme
1003 replacement therapy (ERT) are ineffective or insufficiently effective, when they are available
1004 (MPS-I, II, IV-A, and VI). Difficulties related to ERT is the need for a weekly highly
1005 expensive infusion (~$130,000/year for a child; twice for an adult). Therefore, there is an
1006 imperative need to better understand pathophysiological mechanisms occurring during MPS

1007 disease to tentatively prevent its progression. It was reported that an accumulation of ECM
1008 components in adeno-tonsillar tissue samples of young MPS patients may contribute to the
1009 obstructive phenotype of airway disease (Pal et al., 2018). Nevertheless, the etiopathogenesis
1010 of airway deposits is yet to be elucidated. Few members of the cysteine cathepsin family were
1011 examined in the pathophysiology of MPS during the past years (for review: De Pasquale et
1012 al., 2020). Abnormal expression of cathepsins B, K, and S were reported in tissues of different
1013 MPS animal models (Baldo et al., 2017; Gonzalez et al., 2018; Ohmi et al., 2003; Viana et al.,
1014 2020; Wilson et al., 2009). Their dysregulation may alter both ECM remodeling and
1015 homeostasis of skeletal, cardiac muscles and heart valves. Also, their overexpression was
1016 correlated with growth impairment, joint contractures and cardiovascular disorders found in
1017 animal models. As CatV exhibits *in vitro* the highest elastolytic activity yet described among
1018 mammalian proteases (Yasuda et al., 2004), we focused on CatV expression and activity in
1019 the respiratory secretions of young patients with MPS-I, II and III. CatV was mostly
1020 expressed in alveolar macrophages and bronchial epithelial cells of a MPS-I patient. CatV
1021 was found both as its proform and its mature form in respiratory specimens (sputum and
1022 tracheal aspirates) of MPS patients. However, no significant difference in the expression level
1023 of CatV was observed between MPS and non-MPS groups. Also, CatV levels were similar in
1024 MPS patients irrespective of a weekly ERT (MPS-I and II) or not (MPS-III). Direction for
1025 future research will therefore need to address whether CatV expression is regulated in the
1026 course of progressive lung disorders in a larger cohort of untreated patients with MPS. We
1027 identified HS as the major sulfated GAG ubiquitously found in MPS-I, II, and III specimen
1028 and we established a strong correlation between HS levels and the severity of respiratory-
1029 related disorders. Concomitant to our observations, significant correlations were reported
1030 between the type of accumulated GAGs, including HS, and the relative involvement of
1031 neurological and visceral manifestations in MPS patients (for review: Whitelock & Iozzo,
1032 2005). Thus, high levels of stored HS may be also a useful indicator to predict respiratory
1033 disease severity in young patients with MPS. It should be noticed that despite patients with
1034 MPS-I and II of the present cohort underwent ERT treatment, high HS levels were still
1035 detected compared with healthy controls. ERT had a negligible impact on pulmonary function
1036 in younger children, probably due to limited penetration in the lungs as observed in other
1037 organs (Concolino et al., 2018). On the other hand, the activity of cathepsins is tightly
1038 regulated by linear, negatively charged sulfated Hep, HS, C4-S/C6-S, and DS, unveiling a
1039 pattern of repeating disaccharide units, GlcA/IdoA and a hexosamine, GlcNAc/GalNAc (for
1040 review: Novinec et al., 2014). The overall activity of cathepsins in MPS specimens was

1041 significantly reduced related to *in situ* HS levels, and was negatively correlated with GRSS.
1042 Lack of cathepsin-mediated matrix-degrading activity may affect remodeling of lung tissue in
1043 MPS, as reported either in a mouse model of bleomycin-induced lung fibrosis or sarcoidosis
1044 (Bühling et al., 2004; Samokhin et al., 2011).
1045 Here, we demonstrated that HS-rich MPS sputum and tracheal aspirates inhibited efficiently
1046 CatV activity and that HS could form a stable complex with CatV (K_D=55±5 nM). Moreover,
1047 DS that also accumulated in MPS-I and II inhibited CatV *in vitro*, but not C4-S nor C6-S,
1048 neither of which contains any IdoA in their disaccharide unit. IdoA is the major uronic acid
1049 component of DS and Hep, and in a lesser extent of HS, compared with its epimer β-D-
1050 glucuronic acid (GlcA). However, Hep from porcine intestinal mucosal did not hinder the
1051 peptidase activity of CatV. It is difficult to explain the ineffectiveness of Hep, with a high
1052 level of both sulfation and IdoA, to hinder CatV activity. The low levels of IdoA in the
1053 context of domains with a low level sulfation, common to both HS and DS, may explain their
1054 CatV inhibitory activity.
1055 Numerous reports suggested a role of HS proteoglycans (HSPGs) in the pathogenesis of MPS
1056 (for review: De Pasquale & Pavone, 2019). Here, we used as model the large HSPG perlecan
1057 (~500 kDa), which possesses N-terminal ~65 kDa HS side chains (for review: (Gubbiotti et
1058 al., 2017)). We demonstrated that the inhibition of CatV by perlecan is mediated by its
1059 extended HS chains. Conversely, aggrecan, which mainly possesses CS and KS chains but not
1060 HS, did not impair the peptidase activity of CatV, sustaining the critical role of the HS
1061 moiety. Moreover, low-molecular-weight GAG fragments have been shown to accumulate in
1062 MPS (Fuller et al., 2004). We identified a synthetic HS-derived tetrasaccharide (dp4) that
1063 inhibited potently CatV, suggesting that short oligosaccharides could bind to CatV and impair
1064 its activity. These results are in good agreement with molecular modeling, advocating that dp4
1065 binds within the CatV active site while heparin and C4-S are docked in a region distant from
1066 the active cleft. Furthermore, it was shown that elastolytic activity of CatV was inhibited *in*
1067 *vitro* by the presence of 0.15% DS, but also heparin and C4-S/6-S chains (Yasuda et al.,
1068 2004). This apparent discrepancy is likely due to the fact that elastin degradation by CatV
1069 requires two exosites, which are distant from its active site, and which contribute to elastin
1070 binding and its subsequent cleavage (Du et al., 2013). We found that binding sites of heparin
1071 and C4-S tetrasaccharides are located on a region nearby to one of the identified elastin-
1072 binding exosite (residues Val^{92}-Asn^{104}) and involved in the elastolytic activity of CatV. It can
1073 be speculated that elongation of GAG chains length of heparin and C4-S may hinder the
1074 docking of elastin on this CatV exosite, thus suppressing its enzymatic degradation.

1075 Although human cathepsins V and L encompass a close substrate specificity, CatL activity
1076 towards peptidyl substrates was unchanged in the presence and the absence of 0.15% GAGs
1077 (Li et al., 2000). Docking studies revealed that among residues involved in HS binding, Lys20
1078 of CatV was of peculiar interest. Analysis of human cysteine cathepsin sequences revealed
1079 that a glycine residue is highly conserved in position 20, except for CatW and CatV.
1080 Replacement of the positively charged Lys20 by its counterpart in CatL (Gly20) significantly
1081 decreased the inhibition of the elastolytic activity by HS, supporting that this basic residue is
1082 critical for CatV/HS interactions.
1083 To further address the possibility of an HS antagonist to restore the elastin-degrading activity
1084 of CatV in respiratory specimen of patients with MPS, Surfen was chosen based on its ability
1085 to block HS-dependent activities (Schuksz et al., 2008). Despite the exact mechanism by
1086 which Surfen interacts with HS is unclear, Surfen restored endogenous cathepsin-mediated
1087 elastolytic activity in MPS types I, II and III. Using a series of selective inhibitors of human
1088 cathepsins, we showed that ~40-45% of the total elastolytic activity against Congo Red elastin
1089 can be attributed to both CatB (20%) and CatK (23%). Although CatS was reported to
1090 degrade substantially elastin in monocyte-derived macrophages (Yasuda et al., 2004),
1091 treatment of MPS samples with LHVS did not impair the elastolytic activity. Despite further
1092 studies are needed to investigate the role of CatV in MPS pathogenesis, we may assume that
1093 CatV mostly contributed to the degradation of elastin, which in turn is impaired by the
1094 accumulation of HS in patients with MPS. Accordingly, selective and safe agents (i.e. Surfen
1095 and other HS antagonists) (De Pasquale et al., 2018) preventing HS binding to its molecular
1096 partners could represent an attractive therapeutic option in MPS patients with lung disorders.
1097

1098 **Acknowledgments:**

1099 This work received funding from the French association Vaincre les Maladies Lysosomales
1100 (VML, Massy, France) and was supported by institutional fundings from the Institut National
1101 de la Santé et de la Recherche Médicale (INSERM), the University of Tours and
1102 GagoSciences (Structure, function and regulation of glycosaminoglycans; GDR 3739, Centre
1103 National de la Recherche Scientifique). TC holds a doctoral fellowship from MESRI
1104 (Ministère de l'Enseignement Supérieur, de la Recherche et de l'Innovation, France). SD was
1105 supported by a French Pediatric Society (SFP) award. KKB holds a BMN (Badania Młodych
1106 Naukowców) grant from the Faculty of Chemistry, University of Gdańsk (BMN-538-8370-
1107 B249-18) and a grant (UMO-2018/31/N/ST4/01677) from the National Science Centre of
1108 Poland (Narodowe Cenrtum Nauki). SS received funding (grant UMO-2018/30/E/ST4/00037)

from the National Science Centre of Poland (Narodowe Centrum Nauki). We are grateful to Dr. Florian Mallèvre and Prof. Thierry Livache (Université Grenoble Alpes, CNRS, SPrAM, F-38000 Grenoble, France) for their excellent and skillful assistance in SPRi experiments. Authors acknowledge Prof. Laurent Duca (Université de Reims, Centre National de la Recherche Scientifique (CNRS) 7369, MEDyC, Reims, France) for providing purified bovine neck elastin, Dr. Romain Vivès (Université de Grenoble Alpes, CNRS, Institut de Biologie Structurale, Grenoble, France) for providing the CHO cells, Dr. Michael McDermott (Department of Histopathology, Dublin, Ireland) for providing MPS type I lung tissue samples, and Prof. James McKerrow (Skaggs School of Pharmacy and Pharmaceutical Sciences, University of California, San Diego) for his gift of morpholinourea-leucinyl-homophenylalanine-vinyl-sulfone phenyl inhibitor (LHVS). Authors also acknowledge Dr Julie Chantreuil (Pediatric Intensive Care Unit, University Hospital of Tours, France) for her contribution to sample collection, and patients and their families enrolled in this study.

Author contributions: TC and FL designed research; TC, SD, P-MA, KB, SS, DS, and AS performed research; DB, FZ, RJL, FL, and MT contributed new reagents; TC, SD, KB, DS, SS, GL and FL analyzed data; FL wrote the paper. TC, RJL, DB, P-MA, SS, and GL revised the paper. All authors approved the final version of the manuscript.

Competing interests: The authors declare that they have no competing interests.

References

Adachi, W., Kawamoto, S., Ohno, I., Nishida, K., Kinoshita, S., Matsubara, K., & Okubo, K. (1998). Isolation and characterization of human cathepsin V: a major proteinase in corneal Epithelium. *Investigate Ophtalmology and Visual Science*, *39*(10), 8.

Arn, P., Bruce, I. A., Wraith, J. E., Travers, H., & Fallet, S. (2015). Airway-related symptoms and surgeries in patients With mucopolysaccharidosis I. *Annals of Otology, Rhinology & Laryngology*, *124*(3), 198–205. https://doi.org/10.1177/0003489414550154

Baldo, G., Tavares, A. M. V., Gonzalez, E., Poletto, E., Mayer, F. Q., Matte, U. da S., & Giugliani, R. (2017). Progressive heart disease in mucopolysaccharidosis type I mice may be mediated by increased cathepsin B activity. *Cardiovascular Pathology*, *27*, 45–50. https://doi.org/10.1016/j.carpath.2017.01.001

Barbosa, I., Garcia, S., Barbier-Chassefière, V., Caruelle, JP., Martelly, I., & Papy-Garcia, D. (2003). Improved and simple micro assay for sulfated glycosaminoglycans quantification in biological extracts and its use in skin and muscle tissue studies. *Glycobiology*, *13*(9), 647–653. https://doi.org/10.1093/glycob/cwg082

Barrett, A. J., Kembhavi, A. A., Brown, M. A., Kirschke, H., Knight, C. G., Tamai, M., & Hanada, K. (1982). L- *trans* -Epoxysuccinyl-leucylamido(4-guanidino)butane (E-64) and its analogues as inhibitors of cysteine proteinases including cathepsins B, H and L. *Biochemical Journal*, *201*(1), 189–198. https://doi.org/10.1042/bj2010189

Batzios, S. P., Zafeiriou, D. I., & Papakonstantinou, E. (2013). Extracellular matrix components: an intricate network of possible biomarkers for lysosomal storage disorders? *FEBS Letters*, *587*(8), 1258–1267. https://doi.org/10.1016/j.febslet.2013.02.035

Berger, K. I., Fagondes, S. C., Giugliani, R., Hardy, K. A., Lee, K. S., McArdle, C., Scarpa, M., Tobin, M. J., Ward, S. A., & Rapoport, D. M. (2013). Respiratory and sleep disorders in mucopolysaccharidosis. *Journal of Inherited Metabolic Disease*, *36*(2), 201–210. https://doi.org/10.1007/s10545-012-9555-1

Brömme, D., Li, Z., Barnes, M., & Mehler, E. (1999). Human cathepsin V functional expression, tissue distribution, electrostatic surface potential, enzymatic characterization, and chromosomal localization. *Biochemistry*, *38*(8), 2377–2385. https://doi.org/10.1021/bi982175f

Brömme, D., & Wilson, S. (2011). Role of cysteine cathepsins in extracellular proteolysis. *Extracellular Matrix Degradation*, 23–51. https://doi.org/10.1007/978-3-642-16861-1_2

Bühling, F., Röcken, C., Brasch, F., Hartig, R., Yasuda, Y., Saftig, P., Brömme, D., & Welte, T. (2004). Pivotal role of cathepsin K in lung fibrosis. *The American Journal of Pathology*, *164*(6), 2203–2216. https://doi.org/10.1016/S0002-9440(10)63777-7

Case, D. A., Cerutti, D. S., Cheatham III, T. E., Darden, T. A., & Duke, R. E. (2017). *Amber 2017*.

Choe, Y., Leonetti, F., Greenbaum, D. C., Lecaille, F., Bogyo, M., Brömme, D., Ellman, J. A., & Craik, C. S. (2006). Substrate profiling of cysteine proteases using a combinatorial peptide library identifies functionally unique specificities. *Journal of*

1174 *Biological Chemistry*, *281*(18), 12824–12832.
1175 https://doi.org/10.1074/jbc.M513331200
1176 Chowdhury, S. F., Sivaraman, J., Wang, J., Devanathan, G., Lachance, P., Qi, H., Ménard, R.,
1177 Lefebvre, J., Konishi, Y., Cygler, M., Sulea, T., & Purisima, E. O. (2002). Design of
1178 noncovalent inhibitors of human cathepsin L. From the 96-residue proregion to
1179 optimized tripeptides. *Journal of Medicinal Chemistry*, *45*(24), 5321–5329.
1180 https://doi.org/10.1021/jm020238t
1181 Chung, S., Ma, X., Liu, Y., Lee, D., Tittiger, M., & Ponder, K. P. (2007). Effect of neonatal
1182 administration of a retroviral vector expressing α-l-iduronidase upon lysosomal
1183 storage in brain and other organs in mucopolysaccharidosis I mice. *Molecular*
1184 *Genetics and Metabolism*, *90*(2), 181–192.
1185 https://doi.org/10.1016/j.ymgme.2006.08.001
1186 Concolino, D., Deodato, F., & Parini, R. (2018). Enzyme replacement therapy: efficacy and
1187 limitations. *Italian Journal of Pediatrics*, *44*(S2), Suppl 2 120.
1188 https://doi.org/10.1186/s13052-018-0562-1
1189 De Pasquale, V., Moles, A., & Pavone, L. M. (2020). Cathepsins in the pathophysiology of
1190 mucopolysaccharidoses: new perspectives for therapy. *Cells*, *9*(4), 979.
1191 https://doi.org/10.3390/cells9040979
1192 De Pasquale, V., & Pavone, L. M. (2019). Heparan sulfate proteoglycans: The sweet side of
1193 development turns sour in mucopolysaccharidoses. *Biochimica et Biophysica Acta*
1194 *(BBA) - Molecular Basis of Disease*, *1865*(11), 165539.
1195 https://doi.org/10.1016/j.bbadis.2019.165539
1196 De Pasquale, V., Sarogni, P., Pistorio, V., Cerulo, G., Paladino, S., & Pavone, L. M. (2018).
1197 Targeting Heparan Sulfate Proteoglycans as a Novel Therapeutic Strategy for
1198 Mucopolysaccharidoses. *Molecular Therapy - Methods & Clinical Development*, *10*,
1199 8–16. https://doi.org/10.1016/j.omtm.2018.05.002
1200 Du, X., Chen, N. L. H., Wong, A., Craik, C. S., & Brömme, D. (2013). Elastin degradation by
1201 cathepsin V requires two exosites. *Journal of Biological Chemistry*, *288*(48), 34871–
1202 34881. https://doi.org/10.1074/jbc.M113.510008
1203 Fuller, M., Meikle, P. J., & Hopwood, J. J. (2004). Glycosaminoglycan degradation fragments
1204 in mucopolysaccharidosis I. *Glycobiology*, *14*(5), 443–450.
1205 https://doi.org/10.1093/glycob/cwh049
1206 Gonzalez, E. A., Martins, G. R., Tavares, A. M. V., Viegas, M., Poletto, E., Giugliani, R.,
1207 Matte, U., & Baldo, G. (2018). Cathepsin B inhibition attenuates cardiovascular
1208 pathology in mucopolysaccharidosis I mice. *Life Sciences*, *196*, 102–109.
1209 https://doi.org/10.1016/j.lfs.2018.01.020
1210 Gubbiotti, M. A., Neill, T., & Iozzo, R. V. (2017). A current view of perlecan in physiology
1211 and pathology: a mosaic of functions. *Matrix Biology*, *57–58*, 285–298.
1212 https://doi.org/10.1016/j.matbio.2016.09.003
1213 Gupta, S., O'Meara, A., Wynn, R., & McDermott, M. (2013). Fatal and unanticipated
1214 cardiorespiratory disease in a two-year-old child with Hurler syndrome following
1215 successful stem cell transplant. *JIMD Reports*, *7*, 119–123.
1216 https://doi.org/10.1007/8904_2013_213

1217 Haskins, M. E., Otis, E. J., Hayden, J. E., Jezyk, P. F., & Stramm, L. (1992). Hepatic storage
1218 of glycosaminoglycans in feline and canine models of mucopolysaccharidoses I, VI,
1219 and VII. *Veterinary Pathology*, *29*(2), 112–119.
1220 https://doi.org/10.1177/030098589202900203
1221 Humphrey, W., Dalke, A., & Schulten, K. (1996). VMD: visual molecular dynamics. *Journal*
1222 *of Molecular Graphics*, *14*(1), 33–38. https://doi.org/10.1016/0263-7855(96)00018-5
1223 Iozzo, R. V., & Gubbiotti, M. A. (2018). Extracellular matrix: the driving force of mammalian
1224 diseases. *Matrix Biology*, *71–72*, 1–9. https://doi.org/10.1016/j.matbio.2018.03.023
1225 Kirschner, K. N., Yongye, A. B., Tschampel, S. M., González-Outeiriño, J., Daniels, C. R.,
1226 Foley, B. L., & Woods, R. J. (2008). GLYCAM06: A generalizable biomolecular
1227 force field. Carbohydrates. *Journal of Computational Chemistry*, *29*(4), 622–655.
1228 https://doi.org/10.1002/jcc.20820
1229 Kramer, L., Turk, D., & Turk, B. (2017). The future of cysteine cathepsins in disease
1230 management. *Trends in Pharmacological Sciences*, *38*(10), 873–898.
1231 https://doi.org/10.1016/j.tips.2017.06.003
1232 Lalmanach, G., Saidi, A., Bigot, P., Chazeirat, T., Lecaille, F., & Wartenberg, M. (2020).
1233 Regulation of the proteolytic activity of cysteine cathepsins by oxidants. *International*
1234 *Journal of Molecular Sciences*, *21*(6), 1944. https://doi.org/10.3390/ijms21061944
1235 Lecaille, F., Kaleta, J., & Brömme, D. (2002). Human and parasitic papain-like cysteine
1236 proteases: their role in physiology and pathology and recent developments in inhibitor
1237 design. *Chemical Reviews*, *102*(12), 4459–4488. https://doi.org/10.1021/cr0101656
1238 Leighton, S. E. J., Papsin, B., Vellodi, A., Dinwiddie, R., & Lane, R. (2001). Disordered
1239 breathing during sleep in patients with mucopolysaccharidoses. *International Journal*
1240 *of Pediatric Otorhinolaryngology*, *58*(2), 127–138. https://doi.org/10.1016/S0165-
1241 5876(01)00417-7
1242 Li, Z., Hou, W.-S., & Brömme, D. (2000). Collagenolytic activity of cathepsin K is
1243 specifically modulated by cartilage-resident chondroitin sulfates. *Biochemistry*, *39*(3),
1244 529–536. https://doi.org/10.1021/bi992251u
1245 Liu, R., Xu, Y., Chen, M., Weïwer, M., Zhou, X., Bridges, A. S., DeAngelis, P. L., Zhang, Q.,
1246 Linhardt, R. J., & Liu, J. (2010). Chemoenzymatic design of heparan sulfate
1247 oligosaccharides. *Journal of Biological Chemistry*, *285*(44), 34240–34249.
1248 https://doi.org/10.1074/jbc.M110.159152
1249 Morris, G. M., Goodsell, D. S., Halliday, R. S., Huey, R., Hart, W. E., Belew, R. K., & Olson,
1250 A. J. (1998). Automated docking using a Lamarckian genetic algorithm and an
1251 empirical binding free energy function. *Journal of Computational Chemistry*, *19*(14),
1252 1639–1662. https://doi.org/10.1002/(SICI)1096-987X(19981115)19:14<1639::AID-
1253 JCC10>3.0.CO;2-B
1254 Muenzer, J. (2011). Overview of the mucopolysaccharidoses. *Rheumatology*, *50*(suppl 5), v4–
1255 v12. https://doi.org/10.1093/rheumatology/ker394
1256 Muhlebach, M. S., Wooten, W., & Muenzer, J. (2011). Respiratory manifestations in
1257 mucopolysaccharidoses. *Paediatric Respiratory Reviews*, *12*(2), 133–138.
1258 https://doi.org/10.1016/j.prrv.2010.10.005
1259 Naudin, C., Joulin-Giet, A., Couetdic, G., Plésiat, P., Szymanska, A., Gorna, E., Gauthier, F.,
1260 Kasprzykowski, F., Lecaille, F., & Lalmanach, G. (2011). Human Cysteine Cathepsins

Are Not Reliable Markers of Infection by Pseudomonas aeruginosa in Cystic Fibrosis. *PLoS ONE*, *6*, e25577. https://doi.org/10.1371/journal.pone.0025577

Naumnik, W., Ossolińska, M., Płońska, I., Chyczewska, E., & Nikliński, J. (2014). Endostatin and cathepsin-V in bronchoalveolar lavage fluid of patients with pulmonary sarcoidosis. *Lung Cancer and Autoimmune Disorders*, 55–61. https://doi.org/10.1007/5584_2014_26

Novinec, M., Lenarčič, B., & Turk, B. (2014). Cysteine cathepsin activity regulation by glycosaminoglycans. *BioMed Research International*, *2014*, 1–9. https://doi.org/10.1155/2014/309718

Ohmi, K., Greenberg, D. S., Rajavel, K. S., Ryazantsev, S., Li, H. H., & Neufeld, E. F. (2003). Activated microglia in cortex of mouse models of mucopolysaccharidoses I and IIIB. *Proceedings of the National Academy of Sciences*, *100*(4), 1902–1907. https://doi.org/10.1073/pnas.252784899

Onufriev, A., Case, D. A., & Bashford, D. (2002). Effective Born radii in the generalized Born approximation: the importance of being perfect. *Journal of Computational Chemistry*, *23*(14), 1297–1304. https://doi.org/10.1002/jcc.10126

Pal, A. R., Mercer, J., Jones, S. A., Bruce, I. A., & Bigger, B. W. (2018). Substrate accumulation and extracellular matrix remodelling promote persistent upper airway disease in mucopolysaccharidosis patients on enzyme replacement therapy. *PLOS ONE*, *13*(9), e0203216. https://doi.org/10.1371/journal.pone.0203216

Pan, C., Nelson, M. S., Reyes, M., Koodie, L., Brazil, J. J., Stephenson, E. J., Zhao, R. C., Peters, C., Selleck, S. B., Stringer, S. E., & Gupta, P. (2005). Functional abnormalities of heparan sulfate in mucopolysaccharidosis-I are associated with defective biologic activity of FGF-2 on human multipotent progenitor cells. *Blood*, *106*(6), 1956–1964. https://doi.org/10.1182/blood-2005-02-0657

Panitz, N., Theisgen, S., Samsonov, S. A., Gehrcke, J.-P., Baumann, L., Bellmann-Sickert, K., Köhling, S., Pisabarro, M. T., Rademann, J., Huster, D., & Beck-Sickinger, A. G. (2016). The structural investigation of glycosaminoglycan binding to CXCL12 displays distinct interaction sites. *Glycobiology*, *26*(11), 1209–1221. https://doi.org/10.1093/glycob/cww059

Pichert, A., Samsonov, S. A., Theisgen, S., Thomas, L., Baumann, L., Schiller, J., Beck-Sickinger, A. G., Huster, D., & Pisabarro, M. T. (2012). Characterization of the interaction of interleukin-8 with hyaluronan, chondroitin sulfate, dermatan sulfate and their sulfated derivatives by spectroscopy and molecular modeling. *Glycobiology*, *22*(1), 134–145. https://doi.org/10.1093/glycob/cwr120

Reiser, J., Adair, B., & Reinheckel, T. (2010). Specialized roles for cysteine cathepsins in health and disease. *Journal of Clinical Investigation*, *120*(10), 3421–3431. https://doi.org/10.1172/JCI42918

Rutten, M., Ciet, P., van den Biggelaar, R., Oussoren, E., Langendonk, J. G., van der Ploeg, A. T., & Langeveld, M. (2016). Severe tracheal and bronchial collapse in adults with type II mucopolysaccharidosis. *Orphanet Journal of Rare Diseases*, *11*(1), 50. https://doi.org/10.1186/s13023-016-0425-z

Sage, J., Mallèvre, F., Barbarin-Costes, F., Samsonov, S. A., Gehrcke, J.-P., Pisabarro, M. T., Perrier, E., Schnebert, S., Roget, A., Livache, T., Nizard, C., Lalmanach, G., &

Lecaille, F. (2013). Binding of chondroitin 4-sulfate to cathepsin S regulates its enzymatic activity. *Biochemistry*, *52*(37), 6487–6498. https://doi.org/10.1021/bi400925g

Samokhin, A. O., Gauthier, J. Y., Percival, M. D., & Brömme, D. (2011). Lack of cathepsin activities alter or prevent the development of lung granulomas in a mouse model of sarcoidosis. *Respiratory Research*, *12*(1), 13. https://doi.org/10.1186/1465-9921-12-13

Samsonov, S. A., & Pisabarro, M. T. (2016). Computational analysis of interactions in structurally available protein–glycosaminoglycan complexes. *Glycobiology*, *8*, 850–861.

Santamaría, I., Velasco, G., Cazorla, M., Fueyo, A., Campo, E., & Lã, C. (1998). Cathepsin L2, a novel human cysteine proteinase produced by breast and colorectal carcinomas. *Cancer Res* ., *8*, 1624–1630.

Schuksz, M., Fuster, M. M., Brown, J. R., Crawford, B. E., Ditto, D. P., Lawrence, R., Glass, C. A., Wang, L., Tor, Y., & Esko, J. D. (2008). Surfen, a small molecule antagonist of heparan sulfate. *Proceedings of the National Academy of Sciences*, *105*(35), 13075–13080. https://doi.org/10.1073/pnas.0805862105

Spira, D., Stypmann, J., Tobin, D. J., Petermann, I., Mayer, C., Hagemann, S., Vasiljeva, O., Günther, T., Schüle, R., Peters, C., & Reinheckel, T. (2007). Cell type-specific functions of the lysosomal protease cathepsin L in the heart. *Journal of Biological Chemistry*, *282*(51), 37045–37052. https://doi.org/10.1074/jbc.M703447200

Stapleton, M., Arunkumar, N., Kubaski, F., Mason, R. W., Tadao, O., & Tomatsu, S. (2018). Clinical presentation and diagnosis of mucopolysaccharidoses. *Molecular Genetics and Metabolism*, *125*(1–2), 4–17. https://doi.org/10.1016/j.ymgme.2018.01.003

Tolosa, E., Li, W., Yasuda, Y., Wienhold, W., Denzin, L. K., Lautwein, A., Driessen, C., Schnorrer, P., Weber, E., Stevanovic, S., Kurek, R., Melms, A., & Brömme, D. (2003). Cathepsin V is involved in the degradation of invariant chain in human thymus and is overexpressed in myasthenia gravis. *Journal of Clinical Investigation*, *112*(4), 517–526. https://doi.org/10.1172/JCI200318028

Viana, G. M., Priestman, D. A., Platt, F. M., Khan, S., Tomatsu, S., & Pshezhetsky, A. V. (2020). Brain pathology in mucopolysaccharidoses (MPS) patients with neurological forms. *Journal of Clinical Medicine*, *9*(2), 396. https://doi.org/10.3390/jcm9020396

Vidak, E., Javoršek, U., Vizovišek, M., & Turk, B. (2019). Cysteine cathepsins and their extracellular roles: shaping the microenvironment. *Cells*, *8*(3), 264. https://doi.org/10.3390/cells8030264

Vizovišek, M., Fonović, M., & Turk, B. (2019). Cysteine cathepsins in extracellular matrix remodeling: extracellular matrix degradation and beyond. *Matrix Biology*, *75–76*, 141–159. https://doi.org/10.1016/j.matbio.2018.01.024

Vizovišek, M., Vidak, E., Javoršek, U., Mikhaylov, G., Bratovš, A., & Turk, B. (2020). Cysteine cathepsins as therapeutic targets in inflammatory diseases. *Expert Opinion on Therapeutic Targets*, *24*(6), 573–588. https://doi.org/10.1080/14728222.2020.1746765

Whitelock, J. M., & Iozzo, R. V. (2005). Heparan sulfate: a complex polymer charged with biological activity. *Chemical Reviews*, *105*(7), 2745–2764. https://doi.org/10.1021/cr010213m

Wilson, S., Hashamiyan, S., Clarke, L., Saftig, P., Mort, J., Dejica, V. M., & Brömme, D. (2009). Glycosaminoglycan-mediated loss of cathepsin K collagenolytic activity in MPS I contributes to osteoclast and growth plate abnormalities. *The American Journal of Pathology*, *175*(5), 2053–2062. https://doi.org/10.2353/ajpath.2009.090211

Yasuda, Y., Li, Z., Greenbaum, D., Bogyo, M., Weber, E., & Brömme, D. (2004). Cathepsin V, a novel and potent elastolytic activity expressed in activated macrophages. *Journal of Biological Chemistry*, *279*(35), 36761–36770. https://doi.org/10.1074/jbc.M403986200